Biomaterials 230 (2020) 119574

Contents lists available at ScienceDirect

Biomaterials

journal homepage: www.elsevier.com/locate/biomaterials

Mesenchymal Stromal Cells from Patients with Cyanotic Congenital Heart Disease are Optimal Candidate for Cardiac Tissue Engineering

Kai Kang[a,b,1], Jun-bo Chuai[a,b,1], Bao-dong Xie[a,1], Jian-zhong Li[a,c,1], Hui Qu[d], Hua Wu[a,e], Shao-hong Fang[b], Jin-jin Cui[f], Li-li Xiu[f], Jin-cheng Han[f], Tian-hui Cao[f], Xiao-ping Leng[b,g], Hai Tian[a,b], Ren-Ke Li[h,**], Shu-lin Jiang[a,b,*]

[a] Department of Cardiovascular Surgery, The Second Affiliated Hospital of Harbin Medical University, Harbin, Heilongjiang Province, China
[b] The Key Laboratory of Myocardial Ischemia, Harbin Medical University, Ministry of Education, Heilongjiang Province, China
[c] Department of Thoracic Surgery, The Second Affiliated Hospital of Xi'an Jiao Tong University, Xi'an, Shanxi Province, China
[d] Department of Pediatrics, The Second Affiliated Hospital of Harbin Medical University, Harbin, Heilongjiang Province, China
[e] Department of Thoracic Surgery, The Affiliated Huai'an No.1 People's Hospital of Nanjing Medical University, Huai'an, Jiangsu Province, China
[f] Department of Cardiology, The Second Affiliated Hospital of Harbin Medical University, Harbin, Heilongjiang Province, China
[g] Department of Ultrasound, The Second Affiliated Hospital of Harbin Medical University, Harbin, Heilongjiang Province, China
[h] Department of Surgery and Division of Cardiovascular Surgery, University of Toronto and University Health Network, Toronto, Ontario, Canada

ARTICLE INFO

Keywords:
Cyanotic congenital heart disease
Bone marrow mesenchymal stromal cells
Hypoxia
Tissue engineering
Seeding cells
Cardiac patch

ABSTRACT

Engineered heart tissues (EHTs) are regarded as being the most promising alternative to synthetic materials, and autologous mesenchymal stem cells (MSCs) are widely used as seeding cells. However, few studies have evaluated the feasibility of using MSCs from patients with cyanotic congenital heart disease (C-CHD) as seeding cells for EHTs, in comparison with cells from patients of acyanotic congenital heart disease (A-CHD). In the present study, we cultured MSCs from A-CHD and C-CHD patients in normoxia or hypoxia conditions, and compared their pro-angiogenic, anti-apoptotic and inflammation-modulatory potentials. *In vivo*, we seeded the cells into collagen patches conjugated with, or without, proangiogenic cytokines, which were used to repair the right ventricular outflow tract (RVOT) of rats. The *in vitro* results showed that C-CHD MSCs expressed higher levels of VEGFA and $VEGFR_2$, and secreted more pro-angiogenic and anti-inflammatory cytokines under hypoxic conditions. On the other hand, apoptosis-related genes from C-CHD MSCs were modulated adaptably, converting these cells into an anti-apoptotic phenotype. *In vivo* studies demonstrated that in 4 weeks after RVOT reconstruction, cytokine-immobilized patches seeded with C-CHD MSCs exhibited preserved morphology, prolonged cell survival and enhanced angiogenesis compared to A-CHD MSCs. C-CHD MSCs that undergo "naturally hypoxic precondition" present a better cell source for EHTs, which would provide a promising individualized biomaterial for C-CHD patients.

1. Introduction

Cyanotic congenital heart disease (C-CHD) refers to a group of cardiac structural defects that cause a mixture of oxygenated and unoxygenated blood to occur in systemic circulation. Patients with C-CHD manifest a distinctive bluish-grey appearance and suffer from hypoxia since birth [1]. Currently, most C-CHDs can be surgically corrected during infancy or neonatal periods, owing to advanced surgical techniques [2,3]. Although early surgical interventions have saved numerous children that were previously incurable, some survivors are still at risk for re-operation due to the lack of growth of implanted surgical material. Furthermore, the synthetic material is treated by the patient's immune system as a foreign body, leading to it possibly becoming thrombogenic and infected [4]. Therefore, a new type of material with growth potential is in great demand, in order to overcome the aforementioned current difficulties.

The emergence of engineered heart tissues (EHTs) provides a promising solution because of their potentials to repair and regenerate.

* Corresponding author. The Second Affiliated Hospital of Harbin Medical University, 246 Xue Fu Road, Nangang District, Harbin, Heilongjiang Province, 150086, China.
** Corresponding author. Toronto Medical Discovery Tower, Room 3-702, 101 College St, Toronto, ON, M5G 1L7, Canada.
E-mail addresses: renkeli@uhnresearch.ca (R.-K. Li), jiangshulin111@163.com (S.-l. Jiang).
[1] Equally contributing authors.

https://doi.org/10.1016/j.biomaterials.2019.119574
Received 30 March 2019; Received in revised form 12 September 2019; Accepted 18 October 2019
Available online 06 November 2019
0142-9612/

Although a variety of EHTs have been developed, it still remains far away from clinical application, owing to a series of bottle neck-like challenges [5–7]. For example, despite decades of efforts on pro-angiogenetic strategies [8,9], researchers still struggle with the lacking, as well as the lateness of revascularization within the biomaterials. Additionally, the "optimal" cell source or scaffold for EHTs application has yet to be identified, even though a variety of cells [10,11] and materials [12,13] have been evaluated for this purpose.

Mesenchymal stromal cells (MSCs), as seeding cells, have received great attention for their unique properties of being easy to be isolated and amplified *in vitro* [14], making them feasible for clinical applications. In addition, both the multi-lineage differentiation potential [15] and autologous supply of these cells helps to avoid any immunological and ethical concerns. Furthermore, a large body of experimental and preclinical work have demonstrated the proangiogenic effect of MSCs via paracrine [16], transdifferentation [17,18], or engraftment as pericytes mechanisms [19]. Despite wide recognition of the advantages of MSCs, it remains unclear whether autologous MSCs from patients with C-CHD, who reside in a more hypoxic microenvironment than those from non-C-CHD populations, have a similar therapeutic efficacy as the latter.

As mentioned above, patients with C-CHD suffer from hypoxia since birth, and the biological profiles of MSCs from this special population have not been deeply explored and characterized. The current study is the first report, to our knowledge, that focuses on the therapeutic efficacy of MSCs from C-CHD donors in the tissue engineering field. Clinically, we found that the oxygen tension in the bone marrow of C-CHD patients is lower than that of acyanotic (A)-CHD patients or normal people, which constitutes the "naturally hypoxic sounding" for this kind of hMSCs. Besides, aortopulmonary collateral circulation is generally more abundant in C-CHD patients than those with A-CHD, accompanied by elevated serum vascular endothelial growth factor (VEGF) [20]. This phenomenon has been identified as a protective response of the body to hypoxia, through the HIF/VEGF pathway [21]. It is also known that hypoxic preconditioning improves cell survival after implantation by modulating pro-angiogenic [22], anti-apoptotic and anti-inflammatory [23] gene expression [24]. Of course, it's always a concern that the autologous hMSCs from donors with CHD can't be comparable to cells from normal people due to the inherent genetic defects. While, no solid evidences by far have been proved that the genetic variations causing to CHDs have adverse effects on therapeutic efficacy of cell therapy. Previously, we developed a novel platform through covalently conjugating two pro-angiogenic cytokines (VEGF + bFGF) into a collagen scaffold with 1-ethyl-3-[3-dimethylaminopropyl] carbodiimide hydrochloridechemistry (EDC) [25]. The cytokines conjugated in the patch was released gradually, stimulating cell proliferation *in vitro* and improving cell survival and patch revascularization *in vivo* [26,27]. Thus, we hypothesized that MSCs from C-CHD donors are more pro-angiogenic, anti-apoptotic and -inflammatory after seeding on the patch, due to them having been "preconditioned" in naturally hypoxic surroundings. Furthermore, the immobilized cytokines might interact with the seeded cells, thereby accelerating patch revascularization.

2. Materials and methods

2.1. Bone marrow collection

Bone marrow aspirates were obtained from the sternum of patients undergoing cardiac surgery at the Second Affiliated Hospital of Harbin Medical University. Collection of human bone marrow samples was approved by the Research Ethics Committee of the Second Affiliated Hospital of Harbin Medical University (Ethic Number: 2014-R-010), in conformity with World Medical Association Guidelines. All MSCs were isolated from patients aged 0–5 years old with C-CHD (1.50 ± 1.42 years, N = 30) or A-CHD (1.97 ± 1.18 years, N = 32). The general characteristics of the two groups were listed in Table S1.

2.2. MSCs isolation, culture and passage

Bone marrow mononuclear cells were isolated by centrifugation at 1500 RPM for 20 min with a Ficoll-Paque gradient (1.073 g/mL density; GE Healthcare, Little Chalfont, Buckinghamshire, UK) and seeded into 25 cm^2 culture flasks (Corning, New York, USA) in Iscove's Modified Dulbecco Medium (IMDM, Gibco, Life Technologies, Grand Island, New York, USA) supplemented with 10% fetal bovine serum (FBS, Biological Industries, Kibbutz Beit Haemek, Israel). The cells were incubated at 37 °C under hypoxic (1% O_2, 94% N_2 and 5% CO_2) or normoxic (5% CO_2 and 95% air) atmosphere. Nonadherent cells were removed by refreshing the medium every 3–4 days. The cells were harvested by trypsinization (0.25% trypsin with 0.02% EDTA) and passaged until they reached 80–90% confluence.

2.3. Cell culture condition

MSCs from donors of A-CHD and C-CHD were divided into 4 groups: NA (MSCs from A-CHD donors incubated in normoxic conditions); HA (MSCs from A-CHD donors incubated in hypoxic conditions); NC (MSCs from C-CHD donors incubated in normoxic conditions); HC (MSCs from C-CHD donors incubated in hypoxic conditions). The hypoxic condition was generated using a hypoxic chamber according to the manufacturer's instructions. Briefly, the incubator was flushed with a mixture of gasses (95% N_2 and 5% CO_2) for 3 min, and the chamber was then closed to prevent free flow of exogenous air into the chamber. The final level of oxygen was around 1% (PO_2:12 mmHg, Memmert incubator, Germany). Normoxia refers to conventional conditions, consisting of 5% CO_2 and 95% atmosphere (PO_2:160 mmHg, Heal Force incubator, ShangHai, China). Experiments of anaerobic stress, apoptotic induction and inflammatory cytokines release were performed in an anaerobic incubator (100% N_2, PO_2: 4 mmHg, Plas-Labs, 855-AC, USA). The oxygen pressure in each culture medium is determined by a blood-gas analyzer (GEM Premier 3000, Instrumentation Laboratory, USA) ; at 1 h at least after being placed into respective incubator to permit the full hypoxic levels.

2.4. Proliferation and clonogenic potential of MSCs

Cell Counting Kit-8 (CCK_8; Dojindo, Kumamoto, Japan) was used to determine cell proliferation *in vitro* according to the manufacturer's instructions. Cells were seeded into 96-well plates (Corning Incorporated, Corning, NY, USA) at a primary density of 5000 cells per well. One hundred microlitres of CCK_8 reagent was added to each well at 1, 3, 5, 7, and 9 days of culture. Cells were subsequently incubated for 2 h at 37 °C. The absorbance of each well was measured at 450 nm using a microplate reader (TECAN-Infinite200PRO, Switzerland). Growth curves were plotted and compared.

Colony-forming units (CFUs) assay was used to count the number of colonies under normoxic or hypoxic environment, as previously described [28]. Briefly, cells were plated into six-well plates (1×10^5 cells/well) with MesenCult medium (Stem Cell Technologies, 05420, USA). Two weeks later, cells were stained with Wright-Giemsa staining (Sigma-Aldrich, WG16, USA) in methanol for 5 min at room temperature. Colonies containing ≥ 50 cells were counted.

2.5. In vitro angiogenic assessment of MSCs

ELISA was used to quantify the amount of VEGF, bFGF and PDGF secreted from the cells of each group in the medium supernatant after oxygen/serum deprivation [29]. Briefly, each group of cells were plated in 25 cm^2 culture flasks. When they reached 80% confluence, cells were rinsed twice with PBS, supplemented with serum-free IMDM, and cultured under anaerobic incubator (100% N_2) for 72 h. Medium

supernatant fractions were collected and measured with ELISA kits (VEGF: ab100663; bFGF: ab99979; PDGF: ab184860; all from Abcam, Cambridge, UK) according to the manufacturer's instructions. Total protein of cells in each group was also measured using bicinchoninic acid protein assay kit (BCA, Beyotime, P0010, China). The amount of angiogenic cytokines was expressed as a ratio of the amount of each growth factor and the corresponding total protein (pg/μg).

Protein levels of pro-angiogenic factor-VEGFA and its receptor-$VEGFR_2$ were determined by Western Blotting as previously described [30]. Briefly, cells were lysed with lysis buffer, and protein concentration was measured with a BCA kit according to the manufacturer's protocol. 50 μg of cellular protein from each sample was resolved by SDS-PAGE and transferred to PVDF membranes. Membranes were blocked for 1 h with 5% skim milk and incubated with primary antibodies for VEGFA (Abcam, ab1316) and $VEGFR_2$ (Abcam, ab39256) overnight at 4 °C. Afterwards, membranes were then incubated for 1 h with appropriate secondary antibodies conjugated with horseradish peroxidase and then developed with exposure to chemiluminescence substrates. The developed membranes were photographed with Bio-Rad ChemiDoc XRS equipment (Hercules, CA, USA), then quantified and analyzed using Quantity One software (Hercules).

Tube-formation assay was performed to evaluate the pro-angiogenetic potential of MSCs, as previously described [31]. Briefly, a commercial cell line of human umbilical vein endothelial cells (HUVECs, Cyagen, China) was trypsinized and resuspended in 400 μL IMDM (1.5×10^5/well). Cells were placed in the lower compartment of a 24-well plate (Corning, New York, USA), pre-coated with Matrigel (BD Biosciences, San Jose, CA, USA) for 24 h. Four groups of MSCs (1.5×10^5/well in 400 μL IMDM) were added to the upper chamber inserts with a pore size of 1-μm diameter. HUVECs seeded in the Matrigel-coated plate, without MSC co-culture, was used as the control. After 8 h of incubation at 37 °C, capillary tube structures were observed under phase contrast microscopy (Olympus, Japan), and quantified by counting the number of junction points of the tubes.

2.6. Evaluation of cell apoptosis

To mimic *in vivo* condition, cell apoptosis was induced by oxygen-serum-glucose deprivation, as previously described [29]. In brief, all four groups of MSCs were washed and re-plated with medium without serum and glucose (Life Technologies, 11966025, USA), then incubated in an anaerobic chamber filled with 100% N_2 at 37 °C for 2 h.

Cell apoptosis was determined by Annexin V-FITC/PI Apoptosis Detection Kit (BD Pharmingen, USA), and quantified by flow cytometry. Briefly, after inducing apoptosis, 1×10^5 MSCs of each group were harvested and resuspended in 300 μL binding buffer containing 5 μL Annexin V-FITC for 30 min at 4 °C in the dark, followed by a further incubation with 5 μLPI for 5 min. Samples were then analyzed with a FACSCanto II equipped with FACSDiva Software (BD Bioscience). Live cells were identified as Annexin V-$FITC^-$/PI^- (lower left quadrant), early apoptotic cells as Annexin V-$FITC^+$/PI^- (lower right quadrant), late-stage apoptotic cells as Annexin V-$FITC^+$/PI^+ (upper right quadrant), and necrotic cells as Annexin V-$FITC^-$/PI^+ (upper left quadrant).

TUNEL assay (Roche, Switzerland) was performed to further confirm MSC apoptosis. In brief, cells were plated into a 24-well plate at a primary density of 20,000/well. After apoptosis induction, cells were fixed in 4% paraformaldehyde (PFA) for 30 min, permeabilized with 0.1% Triton X-100 in sodium citrate (1:1000) for 10 min, and then incubated with a mixture of label and enzyme solution (1:10). Nuclei were counter-stained with DAPI (Solarbio, C0060, China). Two single, blinded examiners randomly selected six high-power fields (200 ×) per sample. The percentage of TUNEL positive vs. total cells were counted and calculated.

Cellular protein levels of apoptosis-related factors such as Bcl-2, Bax and Cleaved Caspase-3 in each group were measured with Western Blotting. Western Blotting was performed as described above, and the primary antibodies (Bcl-2: ab32124, Bax: ab182733; Cleaved Caspase-3: ab13585) were all purchased from Abcam Corporation.

2.7. Metabolic activity and inflammatory cytokines expression

Cell metabolic activity was evaluated by measuring the glucose consumption and lactate production using the ELISA kits. Briefly, four groups of hMSCs were seeded into 24-well plates (50000/well, 1 mL medium/well) and cultured in the respective incubators. The supernatants of each group of cells were collected at day3 and day7, and stored at −20 °C. A glucose assay kit (BioAssay Systems, DIGL-200) was used to measure the glucose concentrations with the principle that the absorbance of the newly-formed colored complex with glucose at 630 nm is directly proportional to glucose concentration in the sample. Similarly, the lactate concentrations in the culture medium samples were measured using a lactate assay kit (BioAssay Systems, EFDLC-100) according to manufacturer's instructions and basing on the principle that the tetrazolium salt INT is reduced in a NADH-coupled enzymatic reaction to form a water-soluble formazan color product. The initial glucose concentration was 4.5 g/L and the measures were repeated at the same time on day3, 4,7,8. Thus the amount of glucose consumed or lactate produced in day3 and day7 can be calculated.

The anti- and pro-inflammatory cytokines levels in supernatant of cultured hMSCs were analyzed by ELISA kits (Abcam, Cambridge, UK) for TNF-α (ab181421), IL-1β(ab100562), IL-10(ab46034) or IL-6(ab46027), respectively. In this case, the cell culture condition and the evaluation of released cytokines were identical to that in the aforementionedly anaerobic stress experiment.

2.8. Patch preparation and cell growth kinetics

MSCengineered scaffold was prepared as previously described [25]. Briefly, Ultrafoam collagen sponge (QISHENG, Shanghai, China) sheet was trimmed into uniform scaffolds (diameter: 5 mm, thickness: 2 mm), and immersed in sterile PBS containing 1-Ethyl-3-(3-dimethylaminopropyl) carbodlimide HCl (EDC; Sigma, E7750, 24 mg/mL) and *N*-hydroxysulfosuccinimide (Sulfo-NHS; Pierce Chemicals, 24510, 60 mg/mL) for activation (60 min, room temperature). Some scaffolds were then immersed in a mixed solution of VEGF (Peprotech, 100-20, 1 μg/mL in PBS) and bFGF (Peprotech, 100-18B, 1 μg/mL in PBS) for 2 h for cytokine conjugation, while other scaffolds without cytokines were just immersed in PBS. Thereafter, the two groups of MSCs on those two scaffold groups were cultured in hypoxic incubator, trypsinized, and resuspened in medium volume corresponding to 10 μl per scaffold. Four groups of patches were generated: control patches seeded with HA MSCs (HA), growth factor-conjugated patches seeded with HA MSCs (HA + GF); control patches seeded with HC MSCs (HC), and growth factor-conjugated patches seeded with HC MSCs (HC + GF). Cell suspensions (0.5×10^6/scaffold for CCK8 assay and bromodeoxyuridine [BrdU] staining; 1.0×10^6/scaffold for *in vivo* testing) were evenly seeded into the surface of the scaffolds and incubated for another 40 min (37 °C, 5% CO2), to allow for the cells to attach, followed by addition of 1 mL fresh medium.

Cell growth in scaffolds was measured using CCK_8 assay (Dojindo, Kumamoto, Japan) after 2 and 4 days of hypoxic culture, as described previously [24]. Briefly, scaffolds were put into a 24-well plate and incubated with freshly-prepared CCK_8 labelling solution (10 mg/mL, 500 μL/scaffold) at 37 °C for 4 h. Calibration curve consisted of a blank scaffold (no cells), as well as scaffolds with known number of cells seeded into them (0.2, 0.4, 0.8, and 1.6, $\times 10^6$). Supernatant of both constructs and the standards was removed and transferred into a 96-well; their absorbance in each well was measured at 450 nm using a plate reader (TECAN-Infinite200PRO, Switzerland). The amount of formazan dye formed, as indicated by their absorbance, corresponded to the number of viable, metabolizing cells.

Proliferating cells on scaffolds were identified by BrdU staining

according to the manufacturer's instruction. Briefly, after 24 h of hypoxic cultivation, 10 μM BrdU solution (B8010, Solarbio, China) was added to fresh medium and incubated for another 48 h. Scaffolds were then rinsed with PBS, fixed with 4% PFA, dehydrated, and embedded in optimal cutting temperature compound (OCT, SAKURA, Tissue-Tek, 4583, USA). Frozen sections (5 μm) were sliced and stained with an anti-BrdU antibody (Abcam, ab1893) at 4 °C overnight, followed by secondary antibody (Santa Cruz, sc-2781, USA) incubation for 1 h at room temperature. Nuclei were counter-stained with DAPI. The percentage of proliferating cells was counted by two blinded independent examiners, and results were expressed as the ratio of $BrdU^+$ vs. total cells.

2.9. Experimental animal study

Adult male Sprague-Dawley rats (200–225 g) were obtained from the Experimental Animal Center of the Second Affiliated Hospital of Harbin Medical University. All animal procedures were conducted in accordance with the Guide for the Care and Use of Laboratory Animals (National Institutes of Health Guide, revised 1996) and approved by the Animal Care Committee of the Second Affiliated Hospital of Harbin Medical University. To avoid immune rejection, all rats were given 5 mg/kg cyclosporine A (Novartis, Switzerland) intraperitoneally each day from 3 days before to 28 days after patch implantation.

Surgical procedures were performed as previously described [25]. Briefly, rats were anesthetized by 10% chloral hydrate intraperitoneally (0.3 mL/100 g) and ventilated at 60 cycles/min with a tidal volume of 3 mL. The heart was exposed by a median sternotomy. A purse string suture was performed in the middle of the right ventricular outflow tract (RVOT) free wall, and resected to create a defect about 5 mm in diameter. The right ventricle was repaired with one of the four cell-seeded patches (HA, HA + GF, HC, HC + GF), or with the cell-free but cytokine-conjugated patch (Control). A collagen scaffold was then sutured along the margin of the purse string suture with 7-0 polyprolene to cover the defect. The chest incision was closed in layers with running sutures.

2.10. Morphometric assessment

At 28 days after patch implantation, all animals were sacrificed by injection of 10% KCl into the left ventricle through the cardiac apex. Hearts were removed, and an intraventricular balloon was inserted into the right ventricle. The balloon was filled to 30 mmHg of pressure for photography at fixed distance (50 cm). Patch area was measured using computerized planimetry (Image Pro Plus software, USA) as previously described [4]. Hearts were then fixed in 4% PFA for 48 h, and dehydrated in 10%, 20% and 30% sucrose solution for 1 h, 1 h and 24 h, respectively. Hearts were cut into two parts along the long axis of right ventricular outflow tract, and embedded into OCT compound. After embedding, hearts were sliced into 5 μm thick sections and stained with Masson's trichrome (Sigma-Aldrich, HT15, USA). Patch thickness was measured using computerized planimetry.

2.11. Cell survival and patch revascularization

Immunofluorescence staining was performed to assess cell survival (excluding control patch) and patch revascularization. Briefly, frozen sections (5 μm) from each group of animals were washed 3 times for 15 min with PBS, then permeabilized with 0.1% Triton X-100 in TBS for 1 h and blocked with 5% BSA for 30 min at room temperature in a humidified chamber. Thereafter, each slide was incubated in 100 μL primary antibody against human mitochondria (1:50, Millipore, MAB1273B, USA) or α-smooth muscle actin (α-SMA) (1:100, Abcam, ab7817) at 4 °C overnight, followed by the application of 100 μL of goat anti-mouse IgG-TR antibody (1:200, Santa Cruz, sc-2781) for 1 h at room temperature. Nuclei were counter-stained with DAPI. Slices were then mounted with anti-fading mounting medium (Solarbio, S2110). Under a fluorescence microscope (Nikon Eclipse TE200, Japan), two examiners randomly selected five high-power fields (400 ×) per slide. The number of positive cells or vessels with lumen > 100 μm^2 were calculated and averaged. Moreover, the cross-sectional area of all these vessels per slide was added and normalized by the total tissue area.

2.12. Statistical analysis

All the images were quantified by Image-Pro Plus (Version 6.0, Media Cybernetics, Silver Spring, MD, USA). Result analysis was performed using GraphPad Prism 6 software (GraphPad Software Inc, San Diego, CA, USA). All data were expressed as mean ± SD. Comparison of parameters among 3 or more groups was made with one-way analysis of variance (ANOVA) or two-way ANOVA with repeated measures over time. If the F test was significant ($p < 0.05$), pairwise tests of individual group means were carried out using either the Newman-Keuls or Bonferroni *post-hoc* tests. A p value < 0.05 was considered statistically significant.

3. Results

3.1. Characteristics of cultured MSCs from cyanotic and acyanotic donors

Morphologically, MSCs from cyanotic and acyanotic donors were similar under both hypoxic and normoxic conditions. All cells displayed a homogeneous spindle-shaped population throughout all passages (Fig. 1A). However, cell proliferation differed significantly depending on the cell origin or culture conditions (Fig. 1B). Both “cyanotic” and “acyanotic” MSCs increased more rapidly in hypoxia than that in normoxia. Interestingly, cells from cyanotic donors grew faster than those from acyanotic ones under hypoxic condition. As a result, cell numbers in the HC-group was the highest among the four groups, with a significant difference since day 3 after plating to the end of the observation. The CFU-F assay, which evaluates the numbers of stromal cells in each cell population, showed the similar tendency (Fig. 1C–D). CFU-F numbers were greater in NC than NA, as well as in HC compared to HA groups, In fact, MSCs from the HC-group formed the most CFU-F colonies compared to the other three groups.

3.2. Pro-angiogenetic effect of different MSCs and possible mechanisms

To further explore the possible functional differences between MSCs from C-CHD and A-CHD, we measured the amount of VEGFA protein and its receptor $VEGFR_2$ (FLK-1) in the four cell groups. Western Blotting analysis showed that VEGFA protein level increased significantly when MSCs were cultured under hypoxic conditions compared to their respective normoxic conditions. However, a markedly higher expression of VEGFA were observed in NC than NA, or HC compared to HA. groups (Fig. 2A–B). $VEGFR_2$ expression presented a similar, but less significant profile, among the four groups, with only HC being significantly higher than the HA group (Fig. 2C–D). To examine the possible interaction between VEGFA/$VEGFR_2$ and cell proliferation, we re-plotted the growth curve and measured VEGFA expression when abrogating $VEGFR_2$ with its antagonist (Bevacizumab 500 ng/mL). As showed in Fig. S1 A-C, the proliferation of all four groups of MSCs apparently decreased, with no significant difference among the four groups at any time point, while the VEGFA amount in each cell group followed a similar trend to that of Fig. 2A–B. This data provided direct evidence of a VEGFA/$VEGFR_2$ dependent basis for MSCs proliferation. To further confirm secretion of VEGFA and other possible cytokines, ELISA assay was performed to measure the level of cytokines in the cell culture supernatant from the four groups of MSCs. The results showed that not only VEGFA levels, but also bFGF and PDGF, were markedly higher in HC than in the HA group (Fig. 2E–G). Next, tube formation assay was performed to confirm that increased

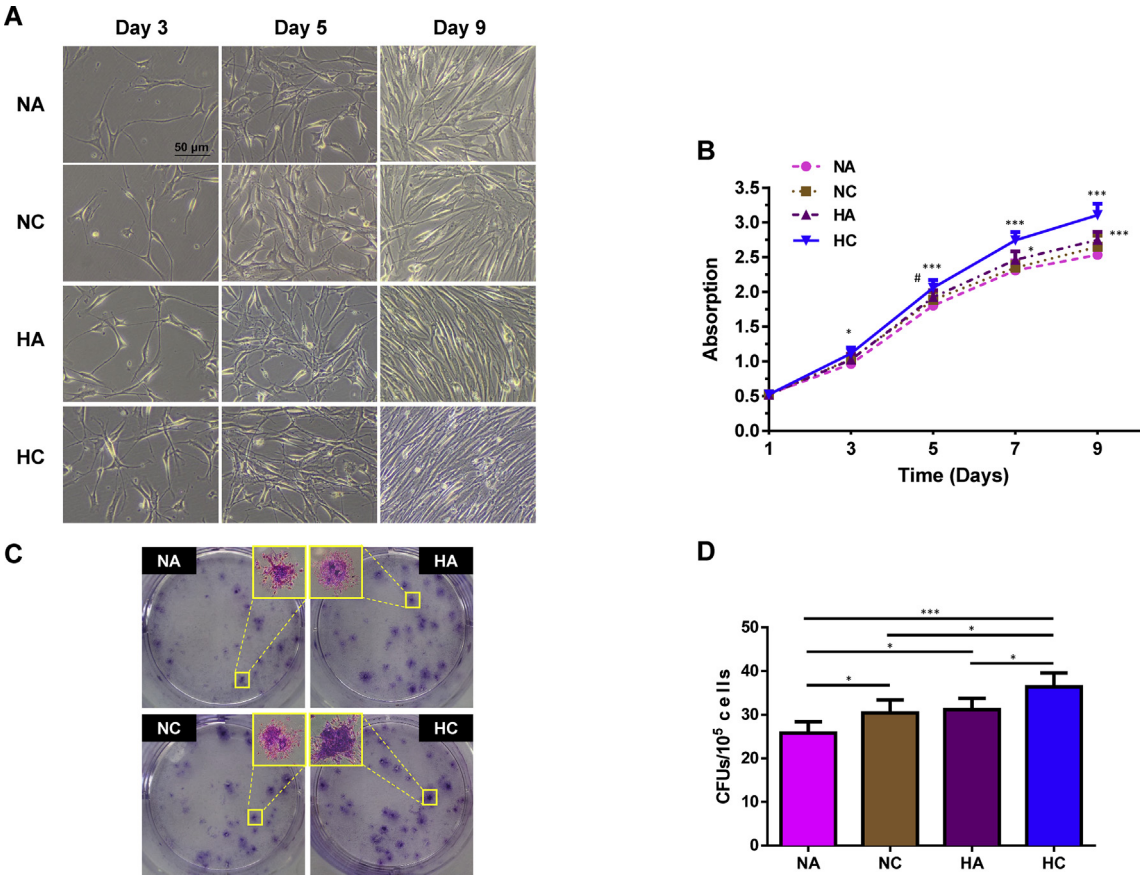

Fig. 1. The proliferation of cultured MSCs from cyanotic or acyanotic donors under normoxic or hypoxic conditions. (A) Representative micrographs (200 ×) of cultured MSCs (Mesenchymal Stromal Cells) at passage 3 at day 3, 5 and 9 after plating. (B) Growth of MSCs was evaluated with Cell Counting Kit-8 (CCK_8) assay at 1, 3, 5, 7 and 9 days after culture. n = 6/group. Day 3: HC vs.NA,*$p < 0.05$, Day 5: HC vs. NC, #$p < 0.01$; HC vs. NA, ***$p < 0.001$; Day 7: HC vs. NC, NA, HA, ***$p < 0.001$; HA vs. NA, *$p < 0.05$; Day 9: HC vs. NC, NA, HA, ***$p < 0.001$; HA vs. NA, ***p < 0.001. (C) Representative photos of CFUs formed by MSCs cultured in colony formation medium (Wright–Giemsa stained). Yellow rectangle indicates amplified CFUs. (D) Quantification of colonies formed from MSCs of cyanotic (C-) or acyanotic (A-) congenital heart disease (CHD) donors cultured under normoxic or hypoxic conditions. n = 5/group. *$p < 0.05$, ***$p < 0.001$. NA: MSCs from A-CHD incubated in normoxic condition; HA: MSCs from A-CHD incubated in hypoxic condition; NC: MSCs from C-CHD incubated in normoxic condition; HC: MSCs from C-CHD incubated in hypoxic condition. CFUs = Colony Forming Units.

secretion of cytokines would result in angiogenesis promotion. The tube formation assay showed that MSCs from all four groups promoted endothelial cells to form capillary-like structures, compared with non-MSC co-cultured controls. Furthermore, as expected, HC-group cells exhibited the highest pro-angiogenetic capability versus the other three groups (Fig. 2H–I).

3.3. Anti-apoptotic ability of different MSCs

To identify whether the “naturally hypoxic preconditioning” improved the anti-apoptotic capacity of MSCs from C-CHD donors, we performed flow cytometry with Annexin V-FITC/PI staining to detect apoptosis extent in each group. Both MSCs cultured under hypoxic condition were more resistant to oxygen-serum-glucose deprivation induced apoptosis than their respective normoxic groups (Fig. 3A–C). However, both early and total apoptosis rate was relatively lower in HC compared to HA groups, with the HC group had the lowest apoptosis rate, indicating that group was the most apoptotic-resistant. A similar outcome was observed in the TUNEL assay (Fig. 3D–E).

To elucidate the mechanism resulting in the apoptotic rate differences, we further examined upstream protein levels of several apoptosis-related genes in the four MSCs groups. As demonstrated in Fig. 3F, hypoxic stimulation significantly upregulated Bcl-2 expression in both HA and HC groups compared to their respective normoxic groups. However, Bcl-2 expression were markedly higher in NC than NA, as well as in HC compared to HA groups. The expression of positive apoptosis regulators Bax and Cleaved Caspase-3 exhibited an opposite response, with hypoxic stimulation having significantly downregulated these molecules in both HA and HC compared to their respective normoxic groups. Furthermore, their expression was markedly lower in NC compared to NA, as well as in HC versus HA groups (Fig. 3G–H). In addition, Bcl-2/Bax ratio, another anti-apoptotic indicator, was found to be the highest in the HC-group, in contrast to the other three groups (Fig. 3I).

3.4. Metabolic profile of different MSCs

Generally, the glucose consumption rate and lactate production rate both increased for all four experimental groups gradually, while the growth speed in each group differed greatly. Specially, the glucose consumption rate was consistently highest in HC group, with a statistically significant difference illustrated in comparison to NA group at day3, and to the other three groups at day7. The production of lactate in each group presented in the similar but less significant pattern (Fig. 4A–B). Furtherly, on a per-cell basis, there were no statistical significance amongst groups for both lactate production and glucose consumption in day3 and day7(Fig. S2 A-B). Thus, any increase in metabolic activities of each group may be attributed to an increase in cell number. The positive linear correlation between cell number and glucose consumption or lactate production rate identified the

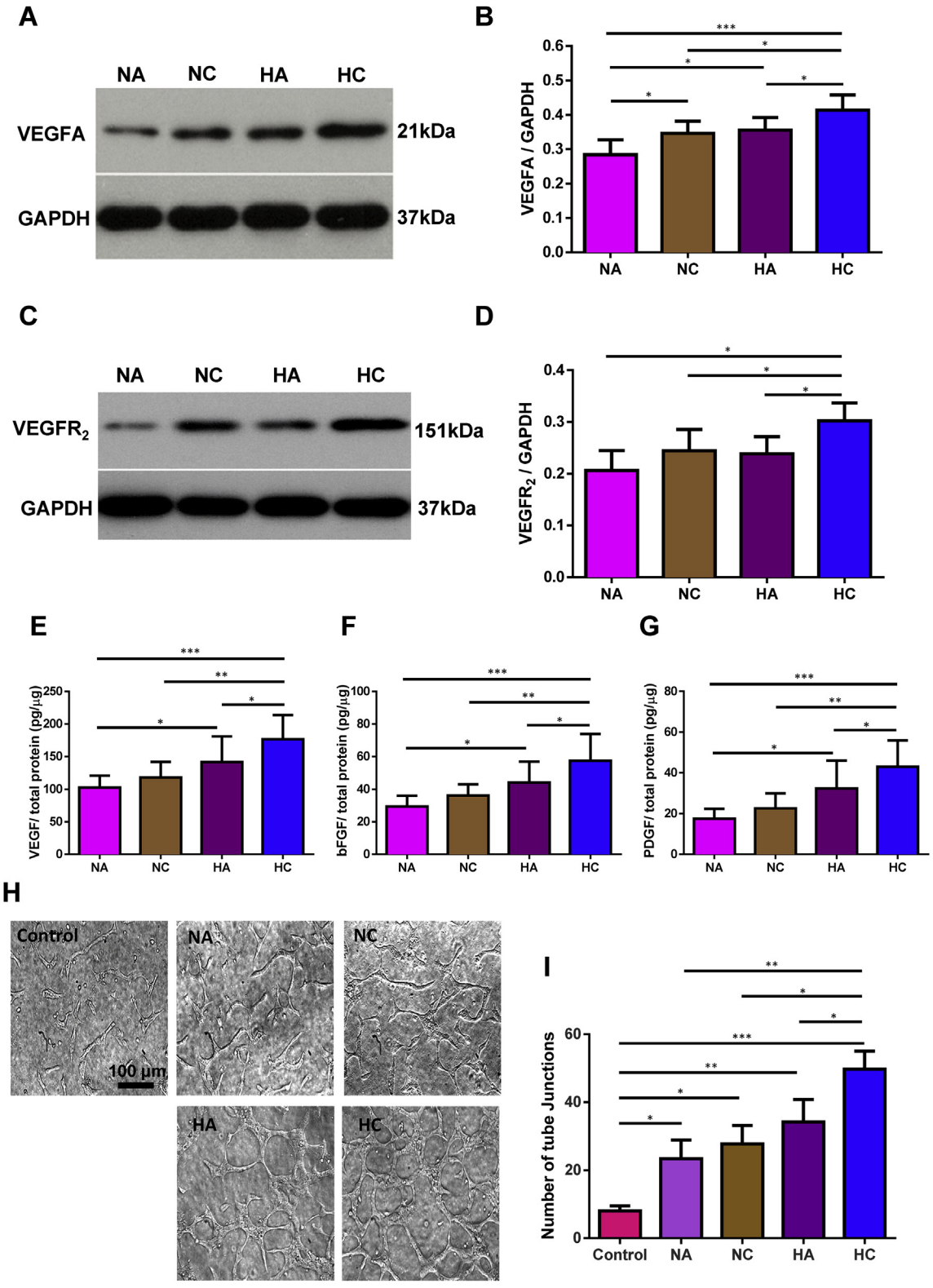

Fig. 2. The proangiogenic capacity of C-CHD MSCs cultured in hypoxia. (A–D) Expression of VEGFA and $VEGFR_2$ in MSCs (Mesenchymal Stromal Cells) from cyanotic (C-) or acyanotic (A-) congenital heart disease (CHD) donors cultured under normoxic or hypoxic conditions was assessed by Western Blotting. GAPDH was used as a loading control. n = 5/group. (E–G) The secretion of VEGF, bFGF and PDGF from C- and A-CHD MSCs cultured in normoxic or hypoxic conditions after serum-oxygen deprivation induction. n = 8/group. (H) Representative photomicrographs showing tube formation of HUVECs co-cultured with different MSCs. (I) Quantitation of the number of endothelial tube junctions demonstrated co-culturing with MSCs promoted HUVECs to form capillary-like structure as compared to HUVECs alone. n = 5/group. $*p < 0.05$, $**p < 0.01$, $***p < 0.001$. VEGFA: vascular endothelial growth factor; $VEGFR_2$: vascular endothelial growth factor receptor 2; bFGF: basic fibroblast growth factor; PDGF: platelet derived growth factor; GAPDH: glyceraldehyde 3-phosphate dehydrogenase; HUVECs: human umbilical vein endothelial cells. NA: MSCs from A-CHD incubated in normoxic condition; HA: MSCs from A-CHD incubated in hypoxic condition; NC: MSCs from C-CHD incubated in normoxic condition; HC: MSCs from C-CHD incubated in hypoxic condition.

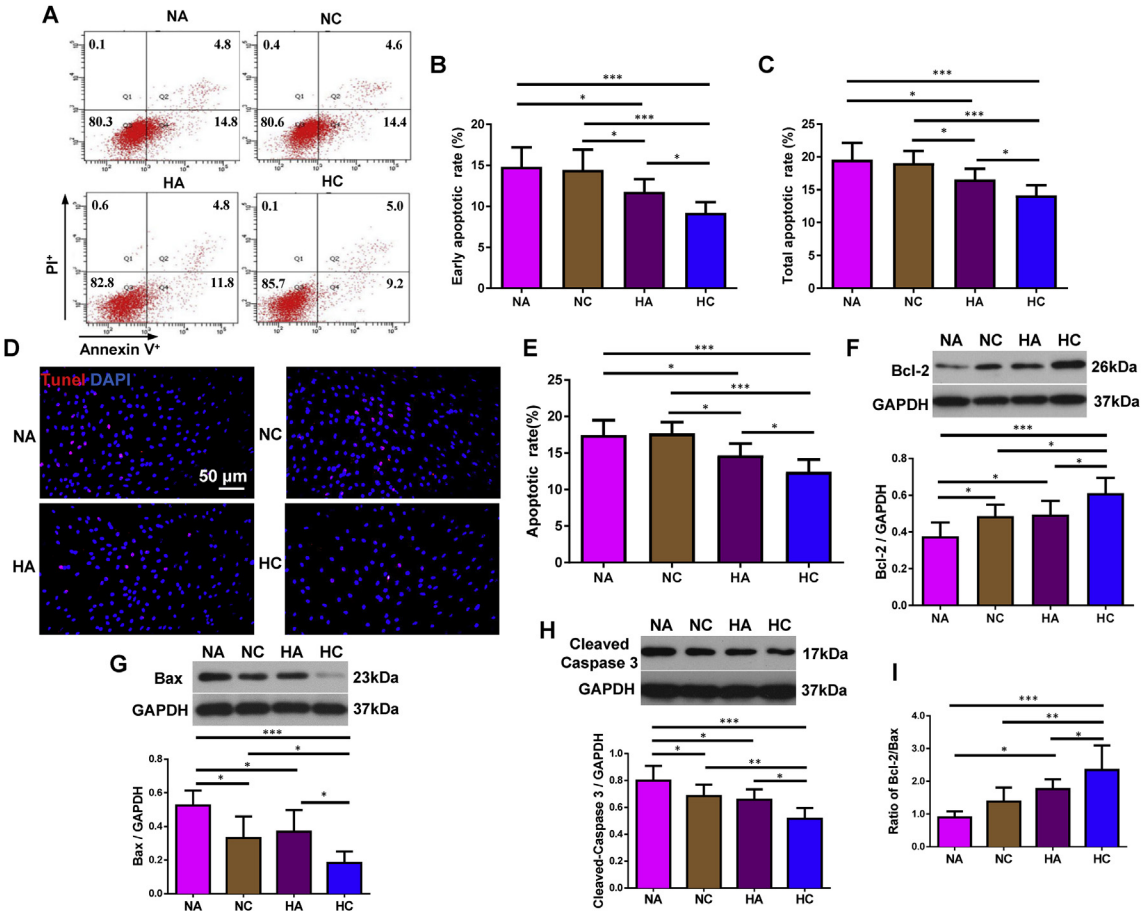

Fig. 3. MSC Apoptosis under oxygen/serum/glucose deprivation *in vitro*. After oxygen-serum-glucose deprivation induction, (A–C) flow cytometry analysis of apoptotic rate in MSCs (Mesenchymal Stromal Cells) from cyanotic (C-) or acyanotic (A-) congenital heart disease (CHD) donors cultured under normoxic or hypoxic conditions. n = 6/group. (D–E) Tunel staining to confirm the apoptotic rate in MSCs from C-CHD and A-CHD donors cultured under normoxic or hypoxic conditions (200 ×). n = 6/group. Western blotting analysis of Bcl-2 (F), Bax (G), Cleaved Caspase-3 (H) protein expression and the ratio of Bcl-2/Bax (I) in MSCs from C-CHD and A-CHD donors cultured under normoxic or hypoxic conditions. GAPDH used as a loading control. n = 6/group. $*p < 0.05$, $**p < 0.01$; $***p < 0.001$; GAPDH: glyceraldehyde 3-phosphate dehydrogenase; Bcl-2: B-cell lymphoma-2. NA: MSCs from A-CHD incubated in normoxic condition; HA: MSCs from A-CHD incubated in hypoxic condition; NC: MSCs from C-CHD incubated in normoxic condition; HC: MSCs from C-CHD incubated in hypoxic condition.

conclusion furtherly (Fig. S2 C-D).

3.5. Anti- and pro-inflammatory cytokines expression of different MSCs

To simulate the inflammatory environment causing by ischemia and hypoxia posterior to transplantation, we cultured all hMSCs in an oxygen-serum deprivation condition and examined the level of inflammation-related cytokines released by cells. As is shown (Fig. 4A–B), in response to such a hypoxia-ischemia-like insult *in vitro*, the production of pro-inflammatory cytokine TNF-α was decreased in both HA and HC groups compared to their respective normoxic groups, and significantly less in HC group compared to the other three groups. IL-1β, another classic pro-inflammatory cytokine, exhibited a less but similar secretory pattern. Whereas, the anti-inflammatory cytokines were secreted in a similar but converse manner, with a significant increase in HC group compared to NA- and NC-group for IL-10 or to the other three groups for IL-6 (Fig. 4C–D). Taken together, hMSCs in HC group produce most anti- and least pro-inflammatory cytokines under the *in vitro* ischemic and hypoxic condition.

3.6. In vitro growth profile of "hypoxic-preconditioned" MSCs in scaffolds with or without cytokine-immobilization

Owing to the beneficial effects of "hypoxic precondition" having been well-documented and verified by our above-mentioned study, we cultured MSCs in scaffolds, with or without cytokine conjugation, under hypoxic conditions. As showed in Fig. 5A, cell numbers increased significantly in both HA + GF and HC + GF groups compared to their respective non-cytokine groups at day 2 and 4 after seeding. Obviously, cytokine addition in scaffolds enhanced cell proliferation. However, cell numbers were markedly higher in HC + GF than HA + GF group at day 4 after seeding, suggesting that MSCs from C-CDH donors seemed to be more sensitive to exogenous cytokine stimulation.

BrdU staining demonstrated a similar tendency, in which $BrdU^+$ cells increased significantly in both HA + GF and HC + GF groups compared to their respective non-cytokine groups (Fig. 5B–C). However, MSCs in the HC + GF scaffold contained the highest $BrdU^+$ number out of the 4 groups, indicating that it had the greatest cell proliferation.

3.7. Preservative effect of seeding cells and tethering cytokines on implanted patch

Next, *in vivo* study was conducted using patches, with or without cytokine-enhancement, that were seeded with MSCs (HA, HC, HA + GF, HC + GF patches), in order to assess their ability to repair rat RVOTs. And the cytokine-immobilized and cell-free patch was used as control. As a thin and dilated patch was closely associated with re-dilation and thus impaired ventricle dysfunction, we focused on the patch morphology after RVOT repair. As demonstrated, patch area increased

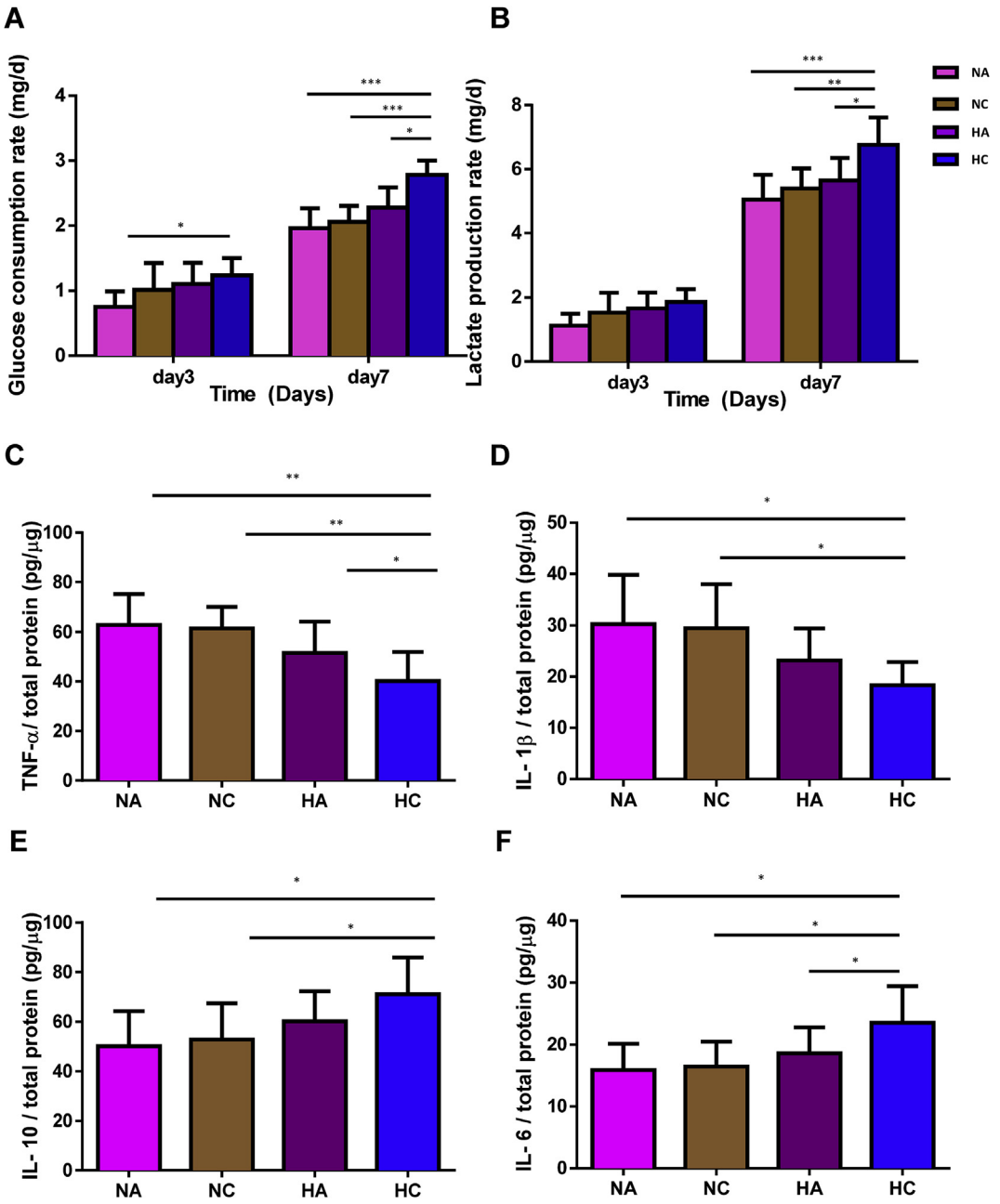

Fig. 4. MSC metabolic ability and the secretion of pro- or anti-inflammatory cytokines under oxygen-serum deprivation. (A–B) Glucose consumption rate and lactate production rate in MSCs (Mesenchymal Stromal Cells) from cyanotic (C-) or acyanotic (A-) congenital heart disease (CHD) donors cultured under normoxic or hypoxic conditions were analyzed by enzyme-linked immunosorbnent assay (ELISA) at day3 and day7 after plating. n = 6/group. (C–F) After serum-oxygen deprivation induction, the secretion of pro-inflammatory cytokines TNF-α, IL-1β and anti-inflammatory cytokines IL-10, IL-6 from C- and A-CHD MSCs cultured in normoxic or hypoxic conditions. n = 8/group. $*p < 0.05$, $**p < 0.01$; $***p < 0.001$. ELISA: enzyme-linked immunosorbnent assay; TNF-α: tumor necrosis factor α; IL-1β: interleukin-6; IL-10: interleukin-10; IL-6: interleukin-6; NA: MSCs from A-CHD incubated in normoxic condition; HA: MSCs from A-CHD incubated in hypoxic condition; NC: MSCs from C-CHD incubated in normoxic condition; HC: MSCs from C-CHD incubated in hypoxic condition.

in all five groups on day 28 compared with that at the time of implantation (Fig. 6A–B). The patch area was comparable among Control, HA, HA + GF and HC groups. However, patch area was smallest in the HC + GF group, at a significantly lower level than for the other four groups. This result indicated that HC-MSCs and cytokines acted synergistically to prevent patch dilation. On the other hand, patch thickness, an indicator of effective RVOT repair, illustrated an opposite trend. At 28 days after implantation, patch thickness in the HC + GF group, as determined by Trichrome staining, was significantly greater than that of the Control or HA group. Although there was no statistical difference, there was still a trend indicating that HC- or HA + GF-patch thickness was greater than that of Control- or HA-patches (Fig. 6C–D). Taken together, these results indicated that HC-MSCs and cytokines acted synergistically to prevent patch dilation.

3.8. *In vivo* cell survival and angiogenesis in scaffolds

Our *in vitro* study had demonstrated the combined beneficial effects of HC-MSCs and cytokine-enhanced scaffolds. Hence, we attempted to confirm that the beneficial effects could be translated into *in vivo* settings. Immunofluorescent staining of heart slices for anti-human specific mitochondria antibody was used to evaluate the survival of seeded

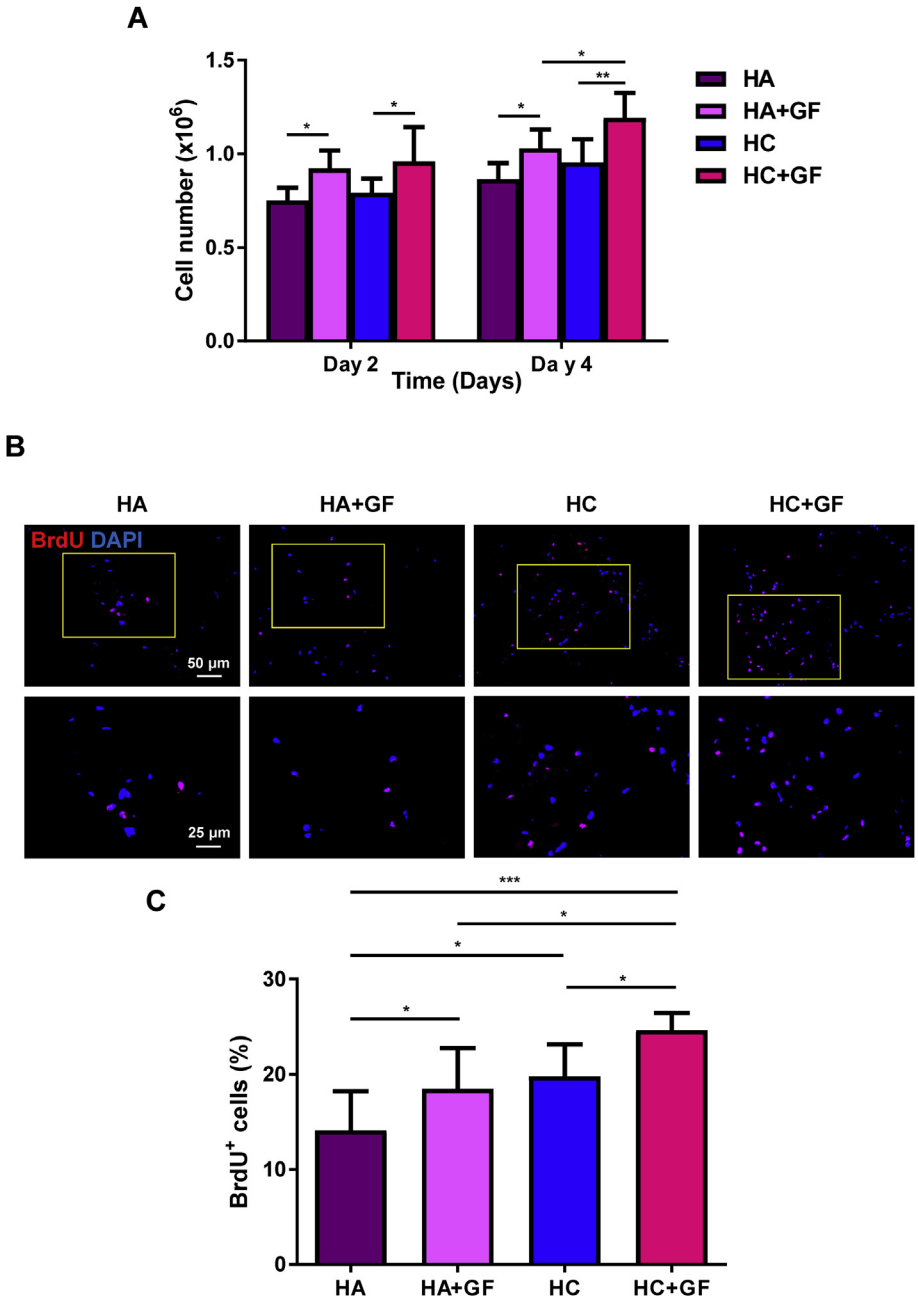

Fig. 5. *In vitro* proliferation of MSCs in scaffold. Collagen scaffolds were conjugated with VEGF and bFGF and seeded with MSCs (Mesenchymal Stromal Cells) from cyanotic (C) or acyanotic (A) congenital heart disease donors under hypoxic (H) condition. Four groups of patches were generated: the control patches seeded with HA MSCs (HA), the growth factor-conjugated patches seeded with HA MSCs (HA + GF); the control patches seeded with HC MSCs (HC), the growth factor-conjugated patches seeded with HC MSCs (HC + GF). (A) Cell numbers were determined by CCK_8 assay in the 4 groups of patches at day 2 and 4 after seeding. n = 6/group. (B) Representative micrographs (200 × and 400 ×) of bromodeoxyuridine (BrdU) staining for proliferating cells. (C) The percentage of $BrdU^+$ cells was quantified in the 4 groups of the patches. Nuclei stained blue with DAPI. n = 8/group. *p < 0.05, **p < 0.01, ***p < 0.001.

cells on the patches at 28 days after patch implantation. The result showed that cell survival was significantly higher in HA + GF and HC + GF compared to their respective non-GF patches. However, HC group cell survival was significantly higher than in the HA group, and was comparable to that of the HA + GF group (Fig. 7A–B). Moreover, cell survival in that HC + GF-patches was the greatest among all four groups.

To evaluate angiogenesis in the patch and around the surrounding tissue, we stained the heart slices for α-SMA to identify newly formed vessels. The vascular density was significantly higher (Fig. 7C–D) in both cytokine-enhanced patches than their corresponding cytokine-free patches, regardless of the seeding cell types. Besides, the vascular density in Control patch was significantly less than that in HA + GF- and HC + GF- patch, but comparable to that in HA- and HC-patch, which illustrating the synergistic effect on patch revascularization of cytokine-enhancement and cell seeding. However, arteriolar density in the HC + GF-patches was the greatest among all five groups. In addition, when angiogenesis was assessed with vessel cross-sectional area, arteriolar cross-sectional area was found to be significantly higher in the HA + GF and HC + GF compared to their respective non-GF groups (Fig. 7E). It is worth noting, though, that arteriolar cross-sectional area in the HC group was significantly higher than the HA group, and was comparable to HA + GF levels. Indeed, arteriolar cross-sectional area in that HC + GF-patches was the biggest among the five groups. All of these results implied that HC MSCs was the ideal seeding cell type, owing to the synergistic actions of MSCs and cytokines, that ultimately maximized the beneficial effects of EHTs.

4. Discussion

The present study evaluated the effects of MSCs from donors of C-CHD vs. A-CHD as seeding cell sources for EHTs. The key finding of this study is that MSCs from patients of C-CHD have the advantages of pro-angiogenesis, anti-apoptosis and anti-inflammation due to their

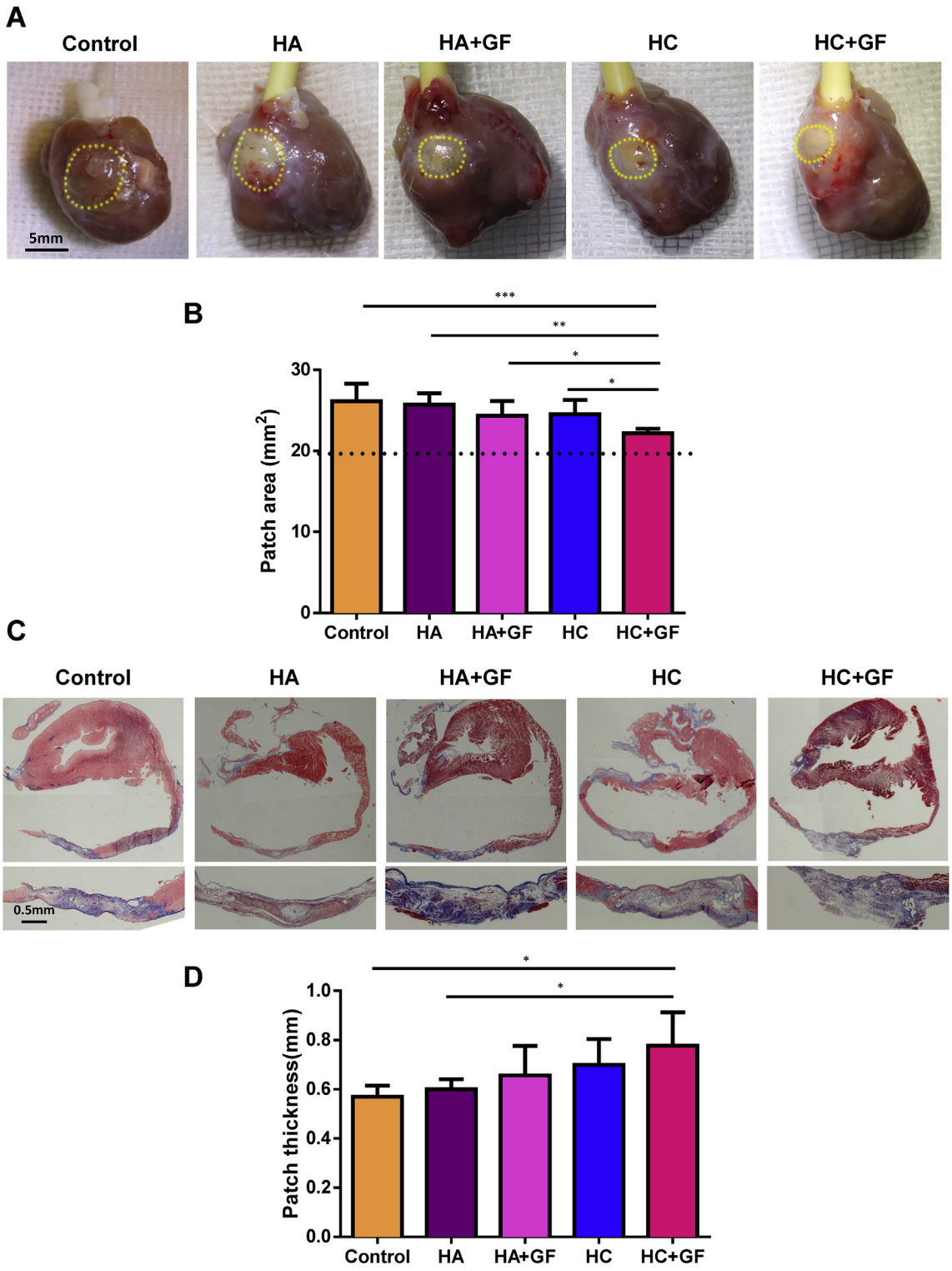

Fig. 6. The area and thickness of patches at 28 days after implantation. Collagen scaffolds were conjugated with VEGF and bFGF and seeded with MSCs (Mesenchymal Stromal Cells) from cyanotic (C) or acyanotic (A) congenital heart disease donors under hypoxic (H) condition or not. Five groups of patches were generated: the growth factor-conjugated patches without cells (Control), the control patches seeded with HA MSCs (HA), the growth factor-conjugated patches seeded with HA MSCs (HA + GF); the control patches seeded with HC MSCs (HC), the growth factor-conjugated patches seeded with HC MSCs (HC + GF). The patches were used to repair the right ventricular outflow tract (RVOT). (A) Representative images of rat hearts showed the outer border of the scaffolds (circled with yellow dotted lines) at 28 days after patch implantation. (B) Patches area was quantified using computerized planimetry. The original patch surface area was around 19.6 mm^2, indicated with the black dotted line. n = 8/group. (C) Representative images of heart slice stained with Masson's trichrome. (D) Patch thickness was quantified using computerized planimetry. All patches had a thickness of 2 mm at the time of implantation and became thinner 28 days later. n = 8/group. *$p < 0.05$, **$p < 0.01$, ***$p < 0.001$. GF: growth factor.

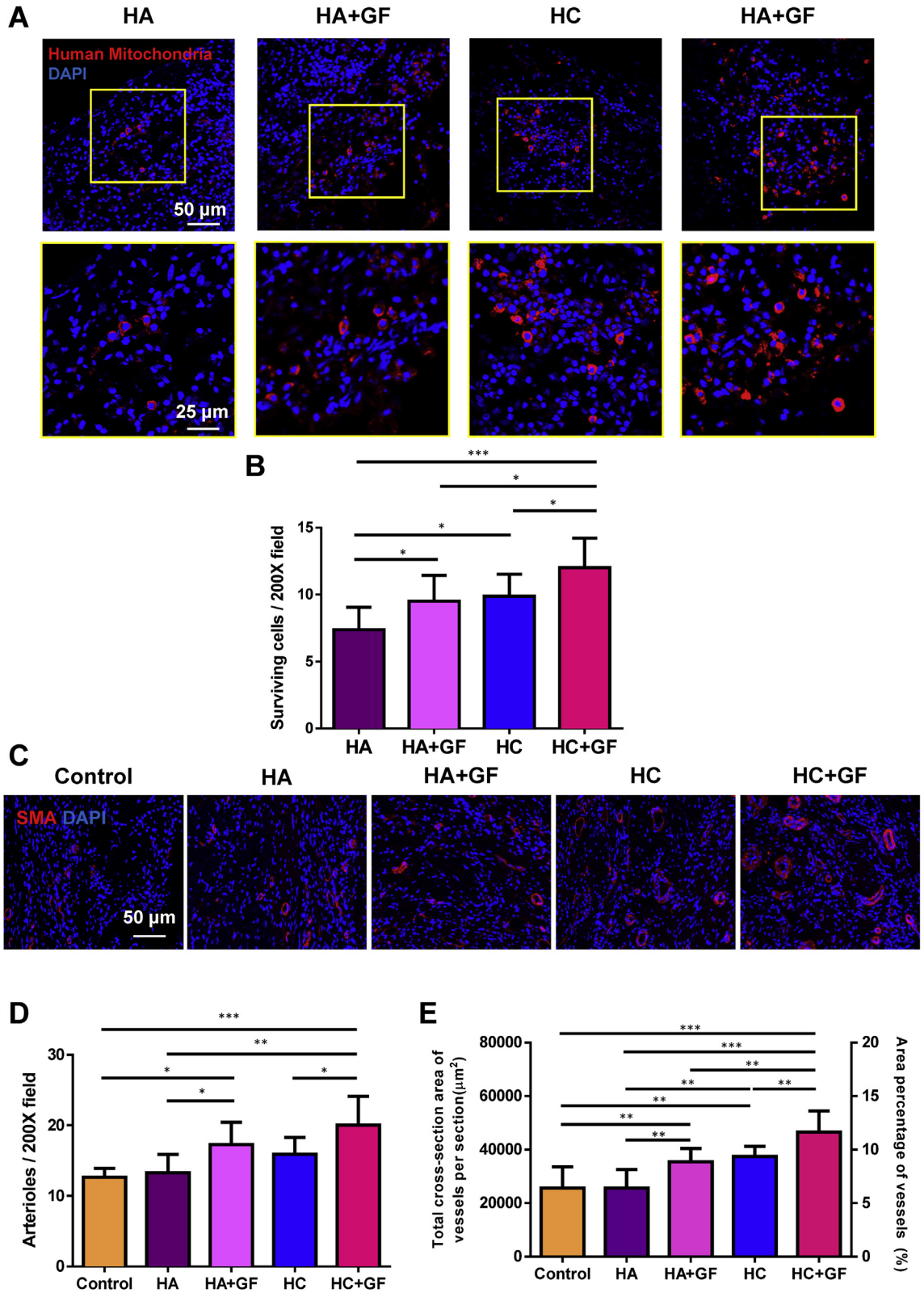

Fig. 7. ***In vivo*** **cell survival and vascular formation in the scaffolds at 28 days after implantation.** Collagen scaffolds were conjugated with VEGF and bFGF and seeded with MSCs (Mesenchymal Stromal Cells) from cyanotic (C) or acyanotic (A) congenital heart disease donors under hypoxic (H) condition or not. Five groups of patches were generated: the growth factor-conjugated patches without cells (Control), the control patches seeded with HA MSCs (HA), the growth factor-conjugated patches seeded with HA MSCs (HA + GF); the control patches seeded with HC MSCs (HC), the growth factor-conjugated patches seeded with HC MSCs (HC + GF). The patches were used to repair the right ventricular outflow tract (RVOT). (A) Representative images of heart slices stained for human specific mitochondria (200 × and 400 ×). (B) Quantification of the number of surviving cells in the patches. n = 8/group. (C) Representative micrographs (200 ×) of immunostaining for α-SMA and DAPI identified arterioles and nuclei, respectively. Quantification of the numbers of arterioles (D) and the total cross-sectional area of vessels (E) in the patches. n = 8/group. $*p < 0.05$, $**p < 0.01$, $***p < 0.001$. α-SMA: alpha smooth muscle actin. GF: growth factor.

"naturally hypoxic precondition", and these cells are therefore a suitable candidate for preparation of individualized autologous EHTs.

To date, a number of experimental and preclinical work have demonstrated the positive effects of MSCs-based therapy, and the enhanced therapeutic efficacy of various MSCs by hypoxic preconditioning [32–35]. Furthermore, a series of clinical trials also evidenced the efficacy and safety of autologous human mesenchymal stem cell [36,37]. However, despite that, for patients with C-CHD, it keeps uncertain whether their hMSCs can be used as seeding cells for cardiac tissue engineering in context of donor-specific personalized cell-therapy. It has been well-documented that C-CHD patients have more abundant collateral vessel formation and higher serum VEGF level than those of A-CHD patients, which can be attributed to the occurrence of hypoxia-induced compensatory angiogenesis [20,38]. This phenomenon led us to postulate that MSCs from C-CHD donors might be more adaptable to hypoxia after cell transplantation due to their "naturally hypoxic preconditioning". Furthermore, these cells might also be able to secrete more cytokines to promote angiogenesis. Indeed, our *in vitro* data on cell growth and colony-formation showed that MSCs from C-CHD cultured under hypoxic conditions exhibited better cell growth and colony formation potentials. Subsequent examinations identified that MSCs cultured under hypoxic conditions have higher VEGFA level than those in normoxic ones. This is consistent with previous findings showing that hypoxia plays an important role in regulating induced VEGF synthesis [21]. More interestingly, MSCs from C-CHD donors were more resistant to apoptosis under hypoxic conditions with serum depravation, as well as having more VEGFA and other cytokine synthesis and secretion, than those from A-CHD donors. What's more, in response to the increased cytokine secretion, co-culture with C-CHD MSCs under hypoxia accelerated endothelial tube formation, with only 8 h of co-culturing needed for HAECs to form well-connected tubular structures. This was in contrast to previous studies showing the need for durations longer than 8 h for HAEC tube formation [39,40]. It is thus plausible that shorter time requirements for endothelial tube formation leads to greater angiogenic effect.

In this study, we identified VEGFA and $VEGFR_2$ as the main mediators of C-CHD MSCs. The VEGF family refers to a group of seven structurally and functionally related cytokines: VEGFA, VEGFB, VEGFC, VEGFD, VEGFE, VEGFF and PIGF. Presently, there is strong evidence that VEGFA plays a major role in angiogenesis. In hypoxic conditions, hypoxia-inducible factor α (HIFα) stimulates VEGFA protein transcription by binding to hypoxia-response element on the VEGFA gene [41]. The resulting VEGFA in circulation can then promote endothelial cell survival, proliferation, migration and differentiation by binding to $VEGFR_1$/FLT_1 and $VEGFR_2$/KDR [42]. Regarding VEGFR, there is agreement that $VEGFR_2$ is the key mediator of mitogenic, angiogenic and permeability-enhancing effects of VEGF [43], via undergoing dimerization and strong ligand-dependent tyrosine phosphorylation. Given the above evidence, we believe that the VEGFA-$VEGFR_2$ signaling represents two targeted molecules involved in C-CHD MSC-mediated angiogenesis.

In considering that angiogenesis is a complex and coordinated process involving numerous molecules, we designed the "hypoxic stress" experiment to identify other possible pro-angiogenic factors that may be involved in C-CHD MSC-mediated angiogenesis. As our data demonstrated, other pro-angiogenic cytokines in addition to VEGF, such as bFGF and PDGF, were also secreted by hypoxic MSCs, and greater cytokine-secreting potential was found in C-CHD MSCs.

Along with pro-angiogenesis, anti-apoptosis capability is also used as a criterion for choosing cells to be seeded. To date, cell apoptosis, especially early apoptosis, is a major factor for limiting the beneficial effects of cell therapy, and often happens as the result of ischemia and hypoxia after cell transplantation [44,45]. Several strategies have been performed to counteract hypoxia-related apoptosis [45,46], and therefore subsequently improve cell therapy efficacy. Increasing evidence strengthen the importance of hypoxic preconditioning in enhancing cellular resistance to hypoxia-induced apoptosis. As Li et al. indicated, anoxic pre-conditioned MSCs achieved improved potency in resisting apoptosis, thereby preserving diabetic cardiomyopathic rat cardiac functioning [47]. A similar result was found by Zhang et al. in mice with myocardial infarction [48]. This decrease of hypoxia-induced apoptosis was identified by Gui et al. to be associated with MSC Bcl-2 up-regulation, as well as Bax and Caspase-3 down-regulation [24]. In agreement with these findings, as is shown in our Annexin V/PI flow cytometry and Tunel staining, MSC apoptotic rate under hypoxic environment is much less than that of corresponding cells cultured in normoxic conditions. More interestingly, MSCs from C-CHD are more resistant to apoptosis than MSCs from A-CHD donors, which we believe is the result of hypoxic preconditioning. These results strengthen our hypothesis that autologous MSCs from C-CHD patients are a better candidate to serve as seeding cells for EHTs.

To further elucidate the molecular mechanism, we revealed that the anti-apoptotic improvement is associated with Bcl-2 up-regulation, as well as Bax and Cleaved Caspase-3 down-regulation. It is well established that Bcl-2 serves as a critical regulator of the pathway involved in apoptosis, acting to inhibit cell death via a distal step in an evolutionarily conserved pathway crucial to apoptosis and programmed cell death. Studies have shown, both in genetically manipulated mouse model and in preclinical and clinical trials, that the accumulation of extra (undead) cells was accompanied with Bcl-2 inhibition [49–51]. By contrast, Bax, the other member of the Bcl-2 family, is a pro-apoptotic gene, inducing apoptosis via forming Bax homodimer or forming a heterodimer with Bcl-2, to antagonizing the latter's anti-apoptotic effect. Therefore, Bcl-2/Bax ratios can be used to assess anti-apoptotic ability in cells [24].

The other major protease enzyme family playing an essential role in apoptosis is caspases. They exist as inactive proenzymes that are sequentially activated during cell apoptosis [52]. It is well-documented that, Caspase-3, especially Cleaved Caspase-3, plays an "executioner" role in both intrinsic and extrinsic apoptotic pathways [53,54]. Accordingly, we can draw the conclusion from our results that MSCs from C-CHD are more resistant to hypoxia-induced apoptosis, probably through Bcl-2 up-regulation, along with Bax and Cleaved Caspase-3 down-regulation.

In addition to ischemia and hypoxia, the inflammatory environment causing by heart damage is another lethal threat to transplanted cells. There is increasing evidence that MSC transplantation may decrease the levels of pro-inflammatory cytokines TNF-α, IL-1β, and/or produce elevated anti-inflammatory cytokines IL-10, IL-6 in response to cardiac injury [55,56], possibly by secreting these cytokines directly, as well as changing the profile of cytokines released by immune cells. Furtherly, the inflammation-modulatory property of MSCs may be enhanced by hypoxia-preconditioning [57,58]. Our data are consistent with these findings. The secretion of pro-inflammatory cytokines TNF-α and IL-1β declined in both MSCs under hypoxic condition, accompanying by the rise of anti-inflammatory cytokines IL-10 and IL-6. Comparatively, hMSCs in HC group proposed higher potential to resist inflammation in response to this ischemia-hypoxia insult. Of note, the improved cell survival of HC-MSCs did not exactly parallel to their anti-inflammatory potential when compared to HA-MSCs, which might be explained as the result of multifactorial improvement of pro-angiogensis and anti-apoptosis, in addition to the anti-inflammatory potential.

Another issue of the present study is the identification of appropriate hypoxic culture conditions. In past decades, various studies were carried out regarding to the optimization of MSCs culture conditions. One point of continuing contention is the ideal oxygen tension is still under debate. Physiological oxygen tension has considerable variation, from as much as 12% in the blood to as low as 1% in the deep zone of cartilage regions [59]. In bone marrow, the oxygen tension of the MSC physiological niche is 2%–7% [60], much lower than in ambient cell culture (21%). Ma et al. have studied the influence of hypoxia on bone marrow–derived MSC behaviors, such as survival, proliferation, and

differentiation, in relation to tissue engineering. Their studies indicated that cellular injury and/or necrosis level under hypoxia was less than that in normoxic condition, owing to normoxic cells being at risk of hyperoxic stress [61]. Their findings were consistent with our results on cell proliferation, metabolism and apoptosis. Additional previous studies have also identified myocardial tissue oxygen tension being around 4% [62]. When myocardial infarction occurs, the oxygen tension of the damaged tissue declines dramatically, ranging from 0.4 to 2.3% [63]. Hypoxia-induced apoptosis can be circumvented by preconditioning the cells in less severe hypoxic conditions (1–3% O_2) for a period of time before exposing them to the more severe hypoxic environment [64]. We speculated that the oxygen concentration in our EHTs may be lower than 4% owing to them lacking vasculature in the early period after transplantation, where the level would be close to that in infarcted tissue. Therefore, we set the oxygen concentration for our *in vitro* culture at 1% to decrease possible hyperoxic injury, and to mimic the *in vivo* oxygen condition after cell transplantation.

To date, a major limitation of cell-seeded cardiac patches is insufficient vasculature within the biomaterial. Therefore, it is widely accepted as an effective measure to modify the cell carrier, in order to accelerate the process of revascularization [65,66]. As the development of a functionally mature vasculature is a dynamic process, requiring multiple cytokines acting sequentially, investigators have exploited a variety of strategies to facilitate the orchestration of cytokines and seeding cells [67]. For example, Dvir T et al. placed their alginate scaffold conjugating prosurvival and proangiogenic cytokines onto the omentum 1 week before implantation. The omental explants showed improved structural and electrical integration with the myocardium and scar tissue after *in vivo* implantation [68]. However, the disadvantages to this "prevascularization strategy" include two additional surgical involvements (implantation and removal) and the temporary cessation of blood flow to the explant prior to implantation. The "scaffold-free approach" refers to produce cardiac tissues by stacking engineered cell sheets, which was developed by Shimizu and others [69,70], wherein the cultured cardiomyocytes (CMs) or endotheliocytes (ECs) monolayers are released as intact cell sheets from a temperature-sensitive culture surface. By manipulating the ratio and assembly of ECs present in the CMs sheets, an increased capillary formation was achieved and donor ECs connected to the host vasculature after implantation. While, as Shimizu et al. showed, the single-step implantation of sheets made from > 3 layers resulted in necrosis for limited diffusion, and repeated implantations of 3-layer cell sheets was necessary to build thick cardiac tissue [71]. Obviously, this approach is impracticable for clinical translation. Additionally, the advancement in microfabrication and microfluidic technologies provide the possibility to generate a physiologically organized microvascular network in scaffolds [72]. For instance, Zheng et al. [73] used photolithographic patterning to create microfluidic channels in high-density collagen gels. After seeding with ECs, these engineered microvessels displayed angiogenic sprouting and perivascular cell recruitment from the bulk collagen to the vessels. Similarly, Choi et al. [74] developed the calcium alginate microfluidic hydrogels with built-in microchannels and systematically studied the diffusion profiles of molecules in the scaffold under pulsed flow at varying flow rates. This microfabrication-based strategy holds the most promising approach to revascularization of cardiac tissues, while the final decision on optimal scaffolds, cells sources and the construction conditions are still in the way. In our previous study, we immobilized VEGF and bFGF into collagen scaffolds using EDC chemistry. The synergistical effect of the controlled release of cytokines rejuvenated old MSCs and accelerated angiogenesis of the cardiac patch induced by seeded MSCs [26]. In the present study, we observed a similar proangiogenic effect for this platform. Moreover, we found that MSCs from the HC-group had greater potential to vascularize the EHTs than MSCs from the HA-group. This was further proved by the result showing that the highest vascular density was present in the HC + GF patch. We believe that the improvement in EHTs angiogenesis as our research identified, should attribute to better modification of the platform, as well as the usage of optimal seeding cells. On the one hand, VEGF and bFGF constant release from the cytokine-enhanced platform might recruit more host endothelial progenitor cells [75], endothelial cells [43] and smooth muscle cells [76] to form the vessel network within or around the bioengineered construct. On the other hand, MSCs from the HC-group were more resistant to post-transplantational hypoxia and inflammation, and had higher capacity to secrete proangiogenic cytokines. This increased angiogenesis enhanced survival of both implanted and recruited cells. Better cell engraftment was associated with the preservation of patch area along with avoidance of ventricular thinning and dilation, which might convert to right ventricular functional improvement.

4.1. Study limitations

The current study was a short-term study that used small animals. Besides, the right ventricular functional assessment was not addressed for technical limitation. So additional long-term studies consisting of more accurate detection means should be performed in pre-setting "cyanotic" large animals caused by right-to-left shunt in cardiac to simulate clinical conditions.

5. Conclusions

In summary, the present study showed the advantages of using MSCs from C-CHD donors as seeding cells for EHTs. These cells were more pro-angiogenic, anti-apoptotic and anti-inflammatory under hypoxic condition due to their naturally hypoxic preconditioning. *In vivo* EHT implantation, established with these cells and cytokine-enhanced (VEGF and bFGF) collagen patches, achieved better revascularization, morphological preservation and cell survival after repairing rat RVOT defects. These novel EHTs provided a promising and individualized biomaterial for C-CHD patients.

Author contributions

KK, J-BC, B-DX, J-ZL and HW performed the research; KK, J-BC and HW participated in data processing and statistical analyses; B-DX, HQ, S–HF, J-JC, L-LX, J-CH, T-HC, X-PL, HT and S-LJ provided experimental technical support; KK, J-BC, B-DX and J-ZL wrote the manuscript; KK, R-KL and S-LJ conceived the research project and drafted the manuscript.

Declaration of competing interest

None.

Acknowledgments

We thank Dr. Shu-Hong Li for help with manuscript preparation and editing. This work was supported by the National Natural Science Foundation of China (81471805, 81871501); Heilongjiang Provincial Science and Technology Research Project (H2018021); Postdoctoral Scientific Research Developmental Fund of Heilongjiang Province (LBH-Q17094); Harbin Municipal Science and Technology Research Fund of Innovative Talents Project (2016RAQXJ139), "Yu Weihan" Outstanding Young Investigator Award (2014) and Earl Bakken Scholarship (2016) to Kai Kang. Support was also provided by Open Research Foundation of Key Laboratory of Myocardial Ischemia (Harbin Medical University, Ministry of Education, China, KF201508) to Jun-bo Chuai.

Appendix B. Supplementary data

Supplementary data to this article can be found online at https://

doi.org/10.1016/j.biomaterials.2019.119574.

Appendix A. Supplementary data

Supplementary data to this article can be found online.

References

[1] N. Kabbani, M.S. Kabbani, H. Al Taweel, Cardiac emergencies in neonates and young infants, Avicenna J. Med. 7 (1) (2017) 1–6.

[2] K. Vitanova, J. Cleuziou, C. Schreiber, T. Gunther, J. Pabst von Ohain, J. Horer, R. Lange, Long-term outcome of patients with complete atrioventricular septal defect combined with the tetralogy of fallot: staged repair is not inferior to primary repair, Ann. Thorac. Surg. 103 (3) (2017) 876–880.

[3] P. Khairy, M. Clair, S.M. Fernandes, E.D. Blume, A.J. Powell, J.W. Newburger, M.J. Landzberg, J.E. Mayer Jr., Cardiovascular outcomes after the arterial switch operation for D-transposition of the great arteries, Circulation 127 (3) (2013) 331–339.

[4] T. Ozawa, D.A. Mickle, R.D. Weisel, N. Koyama, H. Wong, S. Ozawa, R.K. Li, Histologic changes of nonbiodegradable and biodegradable biomaterials used to repair right ventricular heart defects in rats, J. Thorac. Cardiovasc. Surg. 124 (6) (2002) 1157–1164.

[5] P. Kerscher, I.C. Turnbull, A.J. Hodge, J. Kim, D. Seliktar, C.J. Easley, K.D. Costa, E.A. Lipke, Direct hydrogel encapsulation of pluripotent stem cells enables ontomimetic differentiation and growth of engineered human heart tissues, Biomaterials 83 (2016) 383–395.

[6] A. Grosberg, P.W. Alford, M.L. McCain, K.K. Parker, Ensembles of engineered cardiac tissues for physiological and pharmacological study: heart on a chip, Lab Chip 11 (24) (2011) 4165–4173.

[7] J. Riegler, M. Tiburcy, A. Ebert, E. Tzatzalos, U. Raaz, O.J. Abilez, Q. Shen, N.G. Kooreman, E. Neofytou, V.C. Chen, M. Wang, T. Meyer, P.S. Tsao, A.J. Connolly, L.A. Couture, J.D. Gold, W.H. Zimmermann, J.C. Wu, Human engineered heart muscles engraft and survive long term in a rodent myocardial infarction model, Circ. Res. 117 (8) (2015) 720–730.

[8] J.S. Miller, K.R. Stevens, M.T. Yang, B.M. Baker, D.H. Nguyen, D.M. Cohen, E. Toro, A.A. Chen, P.A. Galie, X. Yu, R. Chaturvedi, S.N. Bhatia, C.S. Chen, Rapid casting of patterned vascular networks for perfusable engineered three-dimensional tissues, Nat. Mater. 11 (9) (2012) 768–774.

[9] H. Sekine, T. Shimizu, K. Sakaguchi, I. Dobashi, M. Wada, M. Yamato, E. Kobayashi, M. Umezu, T. Okano, In vitro fabrication of functional three-dimensional tissues with perfusable blood vessels, Nat. Commun. 4 (2013) 1399.

[10] H. Masumoto, T. Matsuo, K. Yamamizu, H. Uosaki, G. Narazaki, S. Katayama, A. Marui, T. Shimizu, T. Ikeda, T. Okano, R. Sakata, J.K. Yamashita, Pluripotent stem cell-engineered cell sheets reassembled with defined cardiovascular populations ameliorate reduction in infarct heart function through cardiomyocyte-mediated neovascularization, Stem cells (Dayton, Ohio) 30 (6) (2012) 1196–1205.

[11] D. Zhang, I.Y. Shadrin, J. Lam, H.Q. Xian, H.R. Snodgrass, N. Bursac, Tissue-engineered cardiac patch for advanced functional maturation of human ESC-derived cardiomyocytes, Biomaterials 34 (23) (2013) 5813–5820.

[12] S. Fleischer, M. Shevach, R. Feiner, T. Dvir, Coiled fiber scaffolds embedded with gold nanoparticles improve the performance of engineered cardiac tissues, Nanoscale 6 (16) (2014) 9410–9414.

[13] A.K. Capulli, L.A. MacQueen, S.P. Sheehy, K.K. Parker, Fibrous scaffolds for building hearts and heart parts, Adv. Drug Deliv. Rev. 96 (2016) 83–102.

[14] V. Karantalis, W. Balkan, I.H. Schulman, K.E. Hatzistergos, J.M. Hare, Cell-based therapy for prevention and reversal of myocardial remodeling, Am. J. Physiol. Heart Circ. Physiol. 303 (3) (2012) H256–H270.

[15] S. Golpanian, A. Wolf, K.E. Hatzistergos, J.M. Hare, Rebuilding the damaged heart: mesenchymal stem cells, cell-based therapy, and engineered heart tissue, Physiol. Rev. 96 (3) (2016) 1127–1168.

[16] S.A. Gomes, E.B. Rangel, C. Premer, R.A. Dulce, Y. Cao, V. Florea, W. Balkan, C.O. Rodrigues, A.V. Schally, J.M. Hare, S-nitrosoglutathione reductase (GSNOR) enhances vasculogenesis by mesenchymal stem cells, Proc. Natl. Acad. Sci. U.S.A. 110 (8) (2013) 2834–2839.

[17] H.C. Quevedo, K.E. Hatzistergos, B.N. Oskouei, G.S. Feigenbaum, J.E. Rodriguez, D. Valdes, P.M. Pattany, J.P. Zambrano, Q. Hu, I. McNiece, A.W. Heldman, J.M. Hare, Allogeneic mesenchymal stem cells restore cardiac function in chronic ischemic cardiomyopathy via trilineage differentiating capacity, Proc. Natl. Acad. Sci. U.S.A. 106 (33) (2009) 14022–14027.

[18] S. Davani, A. Marandin, N. Mersin, B. Royer, B. Kantelip, P. Herve, J.P. Etievent, J.P. Kantelip, Mesenchymal progenitor cells differentiate into an endothelial phenotype, enhance vascular density, and improve heart function in a rat cellular cardiomyoplasty model, Circulation 108 (Suppl 1) (2003) Ii253–I258.

[19] X. Cai, Y. Lin, C.C. Friedrich, C. Neville, I. Pomerantseva, C.A. Sundback, Z. Zhang, J.P. Vacanti, P.V. Hauschka, B.E. Grottkau, Bone marrow derived pluripotent cells are pericytes which contribute to vascularization, Stem Cell Rev. 5 (4) (2009) 437–445.

[20] Y. Mori, M. Shoji, T. Nakanishi, T. Fujii, M. Nakazawa, Elevated vascular endothelial growth factor levels are associated with aortopulmonary collateral vessels in patients before and after the Fontan procedure, Am. Heart J. 153 (6) (2007) 987–994.

[21] P. Carmeliet, Y. Dor, J.M. Herbert, D. Fukumura, K. Brusselmans, M. Dewerchin, M. Neeman, F. Bono, R. Abramovitch, P. Maxwell, C.J. Koch, P. Ratcliffe, L. Moons, R.K. Jain, D. Collen, E. Keshert, Role of HIF-1alpha in hypoxia-mediated apoptosis, cell proliferation and tumour angiogenesis, Nature 394 (6692) (1998) 485–490.

[22] B. Zeng, X. Ren, G. Lin, C. Zhu, H. Chen, J. Yin, H. Jiang, B. Yang, D. Ding, Paracrine action of HO-1-modified mesenchymal stem cells mediates cardiac protection and functional improvement, Cell Biol. Int. 32 (10) (2008) 1256–1264.

[23] T.P. Frazier, J.M. Gimble, I. Kheterpal, B.G. Rowan, Impact of low oxygen on the secretome of human adipose-derived stromal/stem cell primary cultures, Biochimie 95 (12) (2013) 2286–2296.

[24] C. Gui, J.A. Wang, A.N. He, T.L. Chen, R.H. Luo, J. Jiang, X.Y. Hu, X.J. Xie, Heregulin protects mesenchymal stem cells from serum deprivation and hypoxia-induced apoptosis, Mol. Cell. Biochem. 305 (1–2) (2007) 171–178.

[25] Y. Miyagi, L.L. Chiu, M. Cimini, R.D. Weisel, M. Radisic, R.K. Li, Biodegradable collagen patch with covalently immobilized VEGF for myocardial repair, Biomaterials 32 (5) (2011) 1280–1290.

[26] K. Kang, L. Sun, Y. Xiao, S.H. Li, J. Wu, J. Guo, S.L. Jiang, L. Yang, T.M. Yau, R.D. Weisel, M. Radisic, R.K. Li, Aged human cells rejuvenated by cytokine enhancement of biomaterials for surgical ventricular restoration, J. Am. Coll. Cardiol. 60 (21) (2012) 2237–2249.

[27] H. Qu, B.D. Xie, J. Wu, B. Lv, J.B. Chuai, J.Z. Li, J. Cai, H. Wu, S.L. Jiang, X.P. Leng, K. Kang, Improved left ventricular aneurysm repair with cell- and cytokine-seeded collagen patches, Stem Cell. Int. 2018 (2018) 4717802.

[28] J. Yao, S.L. Jiang, W. Liu, C. Liu, W. Chen, L. Sun, K.Y. Liu, Z.B. Jia, R.K. Li, H. Tian, Tissue inhibitor of matrix metalloproteinase-3 or vascular endothelial growth factor transfection of aged human mesenchymal stem cells enhances cell therapy after myocardial infarction, Rejuvenation Res. 15 (5) (2012) 495–506.

[29] X. Song, L. Su, H. Yin, J. Dai, H. Wei, Effects of HSYA on the proliferation and apoptosis of MSCs exposed to hypoxic and serum deprivation conditions, Exp. Ther. Med. 15 (6) (2018) 5251–5260.

[30] Z. Yang, H. Wang, Y. Jiang, M.E. Hartnett, VEGFA activates erythropoietin receptor and enhances VEGFR2-mediated pathological angiogenesis, Am. J. Pathol. 184 (4) (2014) 1230–1239.

[31] B. Zhang, S. Yang, Y. Zhang, Z. Sun, W. Xu, S. Ye, Co-culture of mesenchymal stem cells with umbilical vein endothelial cells under hypoxic condition, J. Huazhong Univ. Sci. Technol. Med. Sci. 32 (2) (2012) 173–180.

[32] B. Antebi, L.A. Rodriguez 2nd, K.P. Walker 3rd, A.M. Asher, R.M. Kamucheka, L. Alvarado, A. Mohammadipoor, L.C. Cancio, Short-term physiological hypoxia potentiates the therapeutic function of mesenchymal stem cells, Stem Cell Res. Ther. 9 (1) (2018) 265.

[33] J. Beegle, K. Lakatos, S. Kalomoiris, H. Stewart, R.R. Isseroff, J.A. Nolta, F.A. Fierro, Hypoxic preconditioning of mesenchymal stromal cells induces metabolic changes, enhances survival, and promotes cell retention in vivo, Stem cells 33 (6) (2015) 1818–1828.

[34] X. Hu, S.P. Yu, J.L. Fraser, Z. Lu, M.E. Ogle, J.A. Wang, L. Wei, Transplantation of hypoxia-preconditioned mesenchymal stem cells improves infarcted heart function via enhanced survival of implanted cells and angiogenesis, J. Thorac. Cardiovasc. Surg. 135 (4) (2008) 799–808.

[35] X. Hu, Y. Xu, Z. Zhong, Y. Wu, J. Zhao, Y. Wang, H. Cheng, M. Kong, F. Zhang, Q. Chen, J. Sun, Q. Li, J. Jin, Q. Li, L. Chen, C. Wang, H. Zhan, Y. Fan, Q. Yang, L. Yu, R. Wu, J. Liang, J. Zhu, Y. Wang, Y. Jin, Y. Lin, F. Yang, L. Jia, W. Zhu, J. Chen, H. Yu, J. Zhang, J. Wang, A large-scale investigation of hypoxia-preconditioned allogeneic mesenchymal stem cells for myocardial repair in nonhuman primates: paracrine activity without remuscularization, Circ. Res. 118 (6) (2016) 970–983.

[36] A.W. Heldman, D.L. DiFede, J.E. Fishman, J.P. Zambrano, B.H. Trachtenberg, V. Karantalis, M. Mushtaq, A.R. Williams, V.Y. Suncion, I.K. McNiece, E. Ghersin, V. Soto, G. Lopera, R. Miki, H. Willens, R. Hendel, R. Mitrani, P. Pattany, G. Feigenbaum, B. Oskouei, J. Byrnes, M.H. Lowery, J. Sierra, M.V. Pujol, C. Delgado, P.J. Gonzalez, J.E. Rodriguez, L.L. Bagno, D. Rouy, P. Altman, C.W. Foo, J. da Silva, E. Anderson, R. Schwarz, A. Mendizabal, J.M. Hare, Transendocardial mesenchymal stem cells and mononuclear bone marrow cells for ischemic cardiomyopathy: the TAC-HFT randomized trial, J. Am. Med. Assoc. 311 (1) (2014) 62–73.

[37] B. Trachtenberg, D.L. Velazquez, A.R. Williams, I. McNiece, J. Fishman, K. Nguyen, D. Rouy, P. Altman, R. Schwarz, A. Mendizabal, B. Oskouei, J. Byrnes, V. Soto, M. Tracy, J.P. Zambrano, A.W. Heldman, J.M. Hare, Rationale and design of the transendocardial injection of autologous human cells (bone marrow or mesenchymal) in chronic ischemic left ventricular dysfunction and heart failure secondary to myocardial infarction (TAC-HFT) trial: a randomized, double-blind, placebo-controlled study of safety and efficacy, Am. Heart J. 161 (3) (2011) 487–493.

[38] W. Himeno, T. Akagi, J. Furui, Y. Maeno, M. Ishii, K. Kosai, T. Murohara, H. Kato, Increased angiogenic growth factor in cyanotic congenital heart disease, Pediatr. Cardiol. 24 (2) (2003) 127–132.

[39] J. Deshane, S. Chen, S. Caballero, A. Grochot-Przeczek, H. Was, S. Li Calzi, R. Lach, T.D. Hock, B. Chen, N. Hill-Kapturczak, G.P. Siegal, J. Dulak, A. Jozkowicz, M.B. Grant, A. Agarwal, Stromal cell-derived factor 1 promotes angiogenesis via a heme oxygenase 1-dependent mechanism, J. Exp. Med. 204 (3) (2007) 605–618.

[40] R. Dong, G.B. Liu, B.H. Liu, G. Chen, K. Li, S. Zheng, K.R. Dong, Targeting long non-coding RNA-TUG1 inhibits tumor growth and angiogenesis in hepatoblastoma, Cell Death Dis. 7 (6) (2016) e2278.

[41] A.K. Olsson, A. Dimberg, J. Kreuger, L. Claesson-Welsh, VEGF receptor signalling - in control of vascular function, Nat. Rev. Mol. Cell Biol. 7 (5) (2006) 359–371.

[42] D.J. Hicklin, L.M. Ellis, Role of the vascular endothelial growth factor pathway in tumor growth and angiogenesis, J. Clin. Oncol. : Off. J. Am. Soc. Clin. Oncol. 23 (5) (2005) 1011–1027.

[43] N. Ferrara, H.P. Gerber, J. LeCouter, The biology of VEGF and its receptors, Nat. Med. 9 (6) (2003) 669–676.

[44] Y.J. Geng, Molecular mechanisms for cardiovascular stem cell apoptosis and growth in the hearts with atherosclerotic coronary disease and ischemic heart failure, Ann. N. Y. Acad. Sci. 1010 (2003) 687–697.
[45] W. Li, N. Ma, L.L. Ong, C. Nesselmann, C. Klopsch, Y. Ladilov, D. Furlani, C. Piechaczek, J.M. Moebius, K. Lutzow, A. Lendlein, C. Stamm, R.K. Li, G. Steinhoff, Bcl-2 engineered MSCs inhibited apoptosis and improved heart function, Stem cells 25 (8) (2007) 2118–2127.
[46] M. Zhang, D. Methot, V. Poppa, Y. Fujio, K. Walsh, C.E. Murry, Cardiomyocyte grafting for cardiac repair: graft cell death and anti-death strategies, J. Mol. Cell. Cardiol. 33 (5) (2001) 907–921.
[47] J.H. Li, N. Zhang, J.A. Wang, Improved anti-apoptotic and anti-remodeling potency of bone marrow mesenchymal stem cells by anoxic pre-conditioning in diabetic cardiomyopathy, J. Endocrinol. Investig. 31 (2) (2008) 103–110.
[48] Z. Zhang, C. Yang, M. Shen, M. Yang, Z. Jin, L. Ding, W. Jiang, J. Yang, H. Chen, F. Cao, T. Hu, Autophagy mediates the beneficial effect of hypoxic preconditioning on bone marrow mesenchymal stem cells for the therapy of myocardial infarction, Stem Cell Res. Ther. 8 (1) (2017) 89.
[49] L. Gandhi, D.R. Camidge, M. Ribeiro de Oliveira, P. Bonomi, D. Gandara, D. Khaira, C.L. Hann, E.M. McKeegan, E. Litvinovich, P.M. Hemken, C. Dive, S.H. Enschede, C. Nolan, Y.L. Chiu, T. Busman, H. Xiong, A.P. Krivoshik, R. Humerickhouse, G.I. Shapiro, C.M. Rudin, Phase I study of Navitoclax (ABT-263), a novel Bcl-2 family inhibitor, in patients with small-cell lung cancer and other solid tumors, J. Clin. Oncol. : Off. J. Am. Soc. Clin. Oncol. 29 (7) (2011) 909–916.
[50] T. Ni Chonghaile, K.A. Sarosiek, T.T. Vo, J.A. Ryan, A. Tammareddi, G. Moore Vdel, J. Deng, K.C. Anderson, P. Richardson, Y.T. Tai, C.S. Mitsiades, U.A. Matulonis, R. Drapkin, R. Stone, D.J. Deangelo, D.J. McConkey, S.E. Sallan, L. Silverman, M.S. Hirsch, D.R. Carrasco, A. Letai, Pretreatment mitochondrial priming correlates with clinical response to cytotoxic chemotherapy, Science (New York, N.Y.) 334 (6059) (2011) 1129–1133.
[51] A.M. Ranger, B.A. Malynn, S.J. Korsmeyer, Mouse models of cell death, Nat. Genet. 28 (2) (2001) 113–118.
[52] Y. Shi, Caspase activation: revisiting the induced proximity model, Cell 117 (7) (2004) 855–858.
[53] G.S. Salvesen, Caspases: opening the boxes and interpreting the arrows, Cell Death Differ. 9 (1) (2002) 3–5.
[54] S. Ghavami, M. Hashemi, S.R. Ande, B. Yeganeh, W. Xiao, M. Eshraghi, C.J. Bus, K. Kadkhoda, E. Wiechec, A.J. Halayko, M. Los, Apoptosis and cancer: mutations within caspase genes, J. Med. Genet. 46 (8) (2009) 497–510.
[55] Y.Y. Du, S.H. Zhou, T. Zhou, H. Su, H.W. Pan, W.H. Du, B. Liu, Q.M. Liu, Immunoinflammatory regulation effect of mesenchymal stem cell transplantation in a rat model of myocardial infarction, Cytotherapy 10 (5) (2008) 469–478.
[56] S. Aggarwal, M.F. Pittenger, Human mesenchymal stem cells modulate allogeneic immune cell responses, Blood 105 (4) (2005) 1815–1822.
[57] A. Saparov, V. Ogay, T. Nurgozhin, M. Jumabay, W.C. Chen, Preconditioning of human mesenchymal stem cells to enhance their regulation of the immune response, Stem Cell. Int. 2016 (2016) 3924858.
[58] Y. Liu, X. Yang, P. Maureira, A. Falanga, V. Marie, G. Gauchotte, S. Poussier, F. Groubatch, P.Y. Marie, N. Tran, Permanently hypoxic cell culture yields rat bone marrow mesenchymal cells with higher therapeutic potential in the treatment of chronic myocardial infarction, Cell. Physiol. Biochem. 44 (3) (2017) 1064–1077.
[59] M. Csete, Oxygen in the cultivation of stem cells, Ann. N. Y. Acad. Sci. 1049 (2005) 1–8.
[60] W.L. Grayson, F. Zhao, R. Izadpanah, B. Bunnell, T. Ma, Effects of hypoxia on human mesenchymal stem cell expansion and plasticity in 3D constructs, J. Cell. Physiol. 207 (2) (2006) 331–339.
[61] T. Ma, W.L. Grayson, M. Frohlich, G. Vunjak-Novakovic, Hypoxia and stem cell-based engineering of mesenchymal tissues, Biotechnol. Prog. 25 (1) (2009) 32–42.
[62] E.G. Mik, T.G. van Leeuwen, N.J. Raat, C. Ince, Quantitative determination of localized tissue oxygen concentration in vivo by two-photon excitation phosphorescence lifetime measurements, J. Appl. Physiol. (Bethesda, Md. : 1985 97 (5) (2004) 1962–1969.
[63] D.J. Ceradini, A.R. Kulkarni, M.J. Callaghan, O.M. Tepper, N. Bastidas, M.E. Kleinman, J.M. Capla, R.D. Galiano, J.P. Levine, G.C. Gurtner, Progenitor cell trafficking is regulated by hypoxic gradients through HIF-1 induction of SDF-1, Nat. Med. 10 (8) (2004) 858–864.
[64] I. Rosova, M. Dao, B. Capoccia, D. Link, J.A. Nolta, Hypoxic preconditioning results in increased motility and improved therapeutic potential of human mesenchymal stem cells, Stem cells 26 (8) (2008) 2173–2182.
[65] Y.L. Chen, C.K. Sun, T.H. Tsai, L.T. Chang, S. Leu, Y.Y. Zhen, J.J. Sheu, S. Chua, K.H. Yeh, H.I. Lu, H.W. Chang, F.Y. Lee, H.K. Yip, Adipose-derived mesenchymal stem cells embedded in platelet-rich fibrin scaffolds promote angiogenesis, preserve heart function, and reduce left ventricular remodeling in rat acute myocardial infarction, Am. J. Tourism Res. 7 (5) (2015) 781–803.
[66] J. Fiedler, K. Breckwoldt, C.W. Remmele, D. Hartmann, M. Dittrich, A. Pfanne, A. Just, K. Xiao, M. Kunz, T. Muller, A. Hansen, R. Geffers, T. Dandekar, T. Eschenhagen, T. Thum, Development of long noncoding RNA-based strategies to modulate tissue vascularization, J. Am. Coll. Cardiol. 66 (18) (2015) 2005–2015.
[67] P.R. Vale, D.W. Losordo, C.E. Milliken, M. Maysky, D.D. Esakof, J.F. Symes, J.M. Isner, Left ventricular electromechanical mapping to assess efficacy of phVEGF (165) gene transfer for therapeutic angiogenesis in chronic myocardial ischemia, Circulation 102 (9) (2000) 965–974.
[68] T. Dvir, A. Kedem, E. Ruvinov, O. Levy, I. Freeman, N. Landa, R. Holbova, M.S. Feinberg, S. Dror, Y. Etzion, J. Leor, S. Cohen, Prevascularization of cardiac patch on the omentum improves its therapeutic outcome, Proc. Natl. Acad. Sci. U.S.A. 106 (35) (2009) 14990–14995.
[69] T. Shimizu, M. Yamato, Y. Isoi, T. Akutsu, T. Setomaru, K. Abe, A. Kikuchi, M. Umezu, T. Okano, Fabrication of pulsatile cardiac tissue grafts using a novel 3-dimensional cell sheet manipulation technique and temperature-responsive cell culture surfaces, Circ. Res. 90 (3) (2002) e40.
[70] H. Sekine, T. Shimizu, K. Hobo, S. Sekiya, J. Yang, M. Yamato, H. Kurosawa, E. Kobayashi, T. Okano, Endothelial cell coculture within tissue-engineered cardiomyocyte sheets enhances neovascularization and improves cardiac function of ischemic hearts, Circulation 118 (14 Suppl) (2008) S145–S152.
[71] T. Shimizu, H. Sekine, J. Yang, Y. Isoi, M. Yamato, A. Kikuchi, E. Kobayashi, T. Okano, Polysurgery of cell sheet grafts overcomes diffusion limits to produce thick, vascularized myocardial tissues, FASEB J. 20 (6) (2006) 708–710.
[72] J.J. Richardson, K. Liang, Nano-biohybrids: in vivo synthesis of metal-organic frameworks inside living plants, Small 14 (3) (2018).
[73] Y. Zheng, J. Chen, M. Craven, N.W. Choi, S. Totorica, A. Diaz-Santana, P. Kermani, B. Hempstead, C. Fischbach-Teschl, J.A. Lopez, A.D. Stroock, In vitro microvessels for the study of angiogenesis and thrombosis, Proc. Natl. Acad. Sci. U.S.A. 109 (24) (2012) 9342–9347.
[74] N.W. Choi, M. Cabodi, B. Held, J.P. Gleghorn, L.J. Bonassar, A.D. Stroock, Microfluidic scaffolds for tissue engineering, Nat. Mater. 6 (11) (2007) 908–915.
[75] E. Shantsila, T. Watson, G.Y. Lip, Endothelial progenitor cells in cardiovascular disorders, J. Am. Coll. Cardiol. 49 (7) (2007) 741–752.
[76] R.D. Kenagy, C.E. Hart, W.G. Stetler-Stevenson, A.W. Clowes, Primate smooth muscle cell migration from aortic explants is mediated by endogenous platelet-derived growth factor and basic fibroblast growth factor acting through matrix metalloproteinases 2 and 9, Circulation 96 (10) (1997) 3555–3560.